

Semiconductors

n, k database

InGaAsP

Equivalents

Si	- Silicon	Ge	- Germanium
GaP	- Gallium Phosphide	GaAs	- Gallium Arsenide
InAs	- Indium Arsenide	C	- Diamond
GaSb	- Gallium Antimonide	InSb	- Indium Antimonide
InP	- Indium Phosphide	GaAs _{1-x} Sb _x	- Gallium Arsenide Antimonide
Al _x Ga _{1-x} As	- Aluminium Gallium Arsenide		
AlN	- Aluminium Nitride	InN	- Indium Nitride
BN	- Boron Nitride	GaN	- Gallium Nitride

We are going to add new data for:

Ga _x In _{1-x} As _y Sb _{1-y}	- Gallium Indium Arsenide Antimonide	Ga _x In _{1-x} P	- Gallium Indium Phosphide
Ga _x In _{1-x} As	- Gallium Indium Arsenide	Ga _x In _{1-x} Sb	- Gallium Indium Antimonide
InAs _{1-x} Sb _x	- Indium Arsenide Antimonide	Ga _x In _{1-x} As _y P _{1-y}	- Gallium Indium Arsenide Phosphide
Si _{1-x} Ge _x	- Silicon Germanium	SiC	- Silicon Carbide

This section is intended to systematize parameters of semiconductor compounds and heterostructures based on them. Such a WWW-archive has a number of advantages: in particular, it enables physicists, both theoreticians and experimentalists, to rapidly retrieve the semiconducting material parameters they are interested in. In addition, physical parameters - optical, electrical, mechanical, etc. - will be presented in the framework of the electronic archive for both the known and new semiconducting compounds. As the starting point in creating the database served the voluminous reference book *"Handbook Series on Semiconductor Parameters"* vol. 1,2 edited by M. Levinstein, S. Rumyantsev and M. Shur, World Scientific, London, 1996, 1999. We express sincere gratitude to M.E. Levinstein for help and attention to this work. A great number of reference books and original papers cited at the end of this section have been used in compiling the information database.

We would like to express our warmest gratitude to all colleagues presented their original data and literature references to complete these archive. If you find these archive pages helpful, and use the data retrieved through the server for your research, we would appreciate acknowledging it in your papers.

We would be indebted very much for any of your further suggestions and comments.

Authors



$Al_x Ga_{1-x} As$

- [Basic Parameters at 300 K](#)
- [Band structure and carrier concentration](#)
- [Electrical Properties](#)
 - [Basic Parameters of Electrical Properties](#)
 - [Mobility and Hall Effect](#)
 - [Two-dimensional electron and hole gas mobility at \$Al_x Ga_{1-x} As/GaAs\$ interface](#)
 - [Transport Properties in High Electric Fields](#)
 - [Transport properties of electron and hole two-dimensional gas in high electric field](#)
 - [Impact Ionization](#)
 - [Recombination Parameters](#)
- [Optical properties](#)
- [Thermal properties](#)
- [Mechanical properties](#)
- [References](#)



Al_xGa_{1-x}As

Basic Parameters at 300 K

Crystal structure	Zinc Blende
Group of symmetry	T _d ² -F43m
Number of atoms in 1 cm ³	(4.42-0.17x)•10 ²²
Debye temperature	370+54x+22x ² K
Density	5.32-1.56x g•cm ⁻³
Dielectric constant (static)	12.90-2.84x
Dielectric constant (high frequency)	10.89-2.73x
Effective electron mass m_e	0.063+0.083x m_o (x<0.45)
Density-of-states electron mass m_{cd}	0.85-0.14x m_o (x>0.45)
Conductivity effective mass m_{cc}	0.26 m_o (x>0.45)
Effective hole masses m_h	0.51+0.25x m_o
Effective hole masses m_{lp}	0.082+0.068x m_o
Electron affinity	4.07-1.1x eV (x<0.45) 3.64-0.14x eV (x>0.45)
Lattice constant	5.6533+0.0078x Å
Optical phonon energy	36.25+1.83x+17.12x ² -5.11x ³ meV



Al_xGa_{1-x}As

Band structure and carrier concentration

[Basic Parameters](#)

[Temperature Dependences](#)

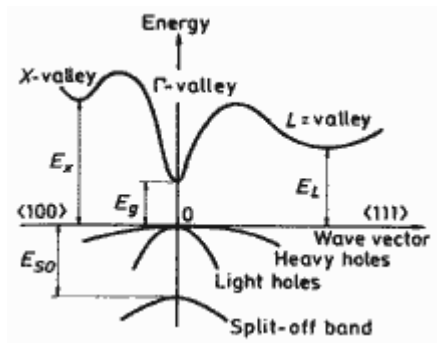
[Dependence on Hydrostatic Pressure](#)

[Energy Gap Narrowing at High Doping Levels](#)

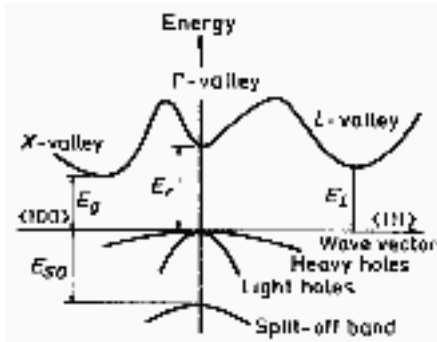
[Band Discontinuities at Al_xGa_{1-x}As/GaAs Heterointerface](#)

Basic Parameters

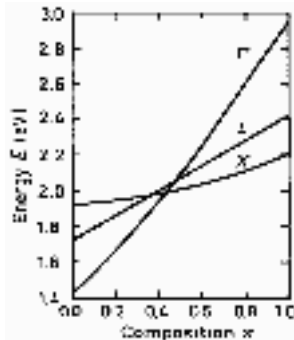
Energy gap	$x < 0.45$	$1.424 + 1.247x$ eV
	$x > 0.45$	$1.9 + 0.125x + 0.143x^2$
Energy separation ($E_{\bullet-L}$) between \bullet and L valleys		0.29 eV
Energy separation (E_{\bullet}) between \bullet and top of valence band		$1.424 + 1.155x + 0.37x^2$ eV
Energy separation (E_X) between X-valley and top of valence band		$1.9 + 0.124x + 0.144x^2$ eV
Energy separation (E_L) between L-valley and top of valence band		$1.71 + 0.69x$ eV
Energy spin-orbital splitting		0.34 - 0.04x eV
Intrinsic carrier concentration	$x = 0.1$	$2.1 \cdot 10^5$ cm ⁻³
	$x = 0.3$	$2.1 \cdot 10^3$ cm ⁻³
	$x = 0.5$	$2.5 \cdot 10^2$ cm ⁻³
	$x = 0.8$	$4.3 \cdot 10^1$ cm ⁻³
Intrinsic resistivity	$x = 0.1$	$4 \cdot 10^9$ $\Omega \cdot \text{cm}$
	$x = 0.3$	$1 \cdot 10^{12}$ $\Omega \cdot \text{cm}$
	$x = 0.5$	$1 \cdot 10^{14}$ $\Omega \cdot \text{cm}$
	$x = 0.8$	$5 \cdot 10^{14}$ $\Omega \cdot \text{cm}$
Effective conduction band density of states	$x < 0.41$	$2.5 \cdot 10^{19} \cdot (0.063 + 0.083x)^{3/2}$ cm ⁻³
	$x > 0.45$	$2.5 \cdot 10^{19} \cdot (0.85 - 0.14x)^{3/2}$ cm ⁻³
Effective valence band density of states		$2.5 \cdot 10^{19} \cdot (0.51 + 0.25x)^{3/2}$ cm ⁻³



Band structure Al_xGa_{1-x} for $x < 0.41-0.45$. Important minima of the conduction band and maxima of the valence band



Band structure Al_xGa_{1-x} for $x > 0.45$. Important minima of the condition band and maxima of the valence band



Energy separation between \bullet -, X-, and L- conduction band minima and top of the valence band versus composition.

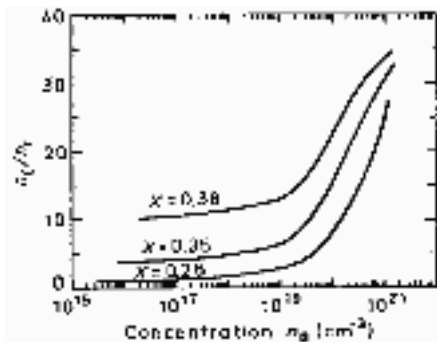
Crossover points:

$$x_c(L-X) = 0.35 \text{ eV} \quad E_L = E_X = 1.95 \text{ eV}$$

$$x_c(\bullet-X) = 0.41 \text{ eV} \quad E_\bullet = E_X = 1.97 \text{ eV}$$

$$x_c(\bullet-L) = 0.47 \text{ eV} \quad E_\bullet = E_L = 2.04 \text{ eV}$$

([Saxena \[1980\]](#)).



Ratio of the total carrier concentration to the carrier concentration in \bullet -valley as a function of equilibrium carrier concentration at 300K

([Zarem et al. \[1989\]](#)).

Temperature Dependences

To estimate the temperature dependences of energy difference between the top of the valence band and the bottom of the \bullet , X, and L valleys of the conduction band E_\bullet , E_X and E_L one can use the data for GaAs ([Aspnes \[1976\]](#)).

$$E_\bullet = E_\bullet(0) - 5.41 \cdot 10^{-4} \cdot T^2 / (T + 204) \text{ (eV)}$$

$$\text{where } E_\bullet(0) = 1.519 + 1.155x + 0.37x^2 \text{ (eV)}$$

$$E_X = E_X(0) - 4.6 \cdot 10^{-4} \cdot T^2 / (T + 204) \text{ (eV)}$$

$$\text{where } E_X(0) = 1.981 + 0.124x + 0.144x^2 \text{ (eV)}$$

$$E_L = E_L(0) - 6.05 \cdot 10^{-4} \cdot T^2 / (T + 204) \text{ (eV)}$$

$$\text{where } E_L(0) = 1.815 + 0.069x \text{ (eV)}$$

Temperature dependence of the energy difference between the top of the valence band and the bottom of the L-valley of the conduction band

$$E_L = 1.815 - 6.05 \cdot 10^{-4} \cdot T^2 / (T + 204) \text{ (eV)}$$

Temperature dependence of the energy difference between the top of the valence band and the bottom of the X-valley of the conduction band

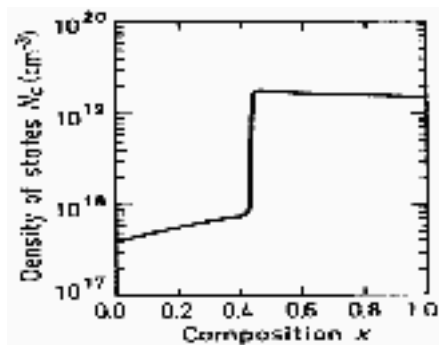
$$E_L = 1.981 - 4.60 \cdot 10^{-4} \cdot T^2 / (T + 204) \text{ (eV)}$$

Effective density of states in the conduction band N_c

$$X < 0.41 \quad N_c = 4.82 \cdot 10^{15} \cdot (m \cdot / m_0)^{3/2} \cdot T^{3/2} = 4.82 \cdot 10^{15} \cdot T^{3/2} \cdot (0.063 + 0.083x)^{3/2} \text{ (cm}^{-3}\text{)}$$

$$X > 0.41 \quad N_c = 4.82 \cdot 10^{15} \cdot (m_{cd}/m_0)^{3/2} \cdot T^{3/2} = 4.82 \cdot 10^{15} \cdot T^{3/2} \cdot (0.85 - 0.14x)^{3/2} \text{ (cm}^{-3}\text{)}$$

where m_{cd} is effective mass of the density of states;

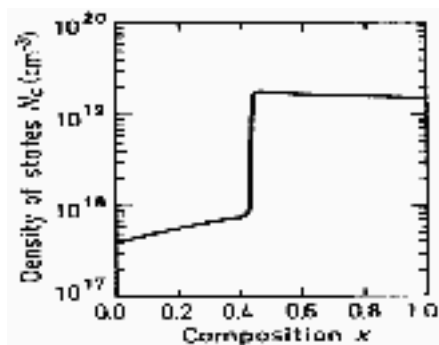


Effective density of states in the conduction band versus x.
(Calculated)

Effective density of states in the valence band N_v

$$N_v = 4.82 \cdot 10^{15} \cdot T^{3/2} \cdot (0.51 + 0.25x)^{3/2} \text{ (cm}^{-3}\text{)} \quad X > 0.41 \quad N_c = 4.82 \cdot 10^{15} \cdot (m_{cd}/m_0)^{3/2} \cdot T^{3/2} =$$

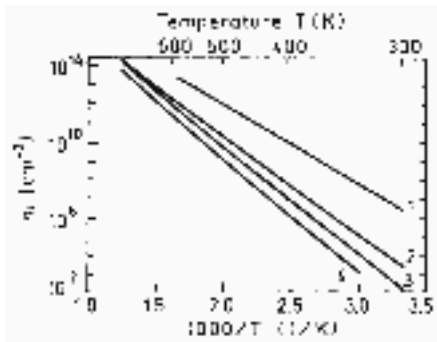
$$4.82 \cdot 10^{15} \cdot T^{3/2} \cdot (0.85 - 0.14x)^{3/2} \text{ (cm}^{-3}\text{)}$$



Effective density of states in the conduction band versus x.
(Calculated)

Intrinsic Carrier Concentration

$$n_i = (N_c \cdot N_v)^{1/2} \exp[-E_g / (2k_b T)]$$



The temperature dependences of the intrinsic carrier concentration.

1. $x=0$
2. $x=0.3$
3. $x=0.6$
4. $x=1$

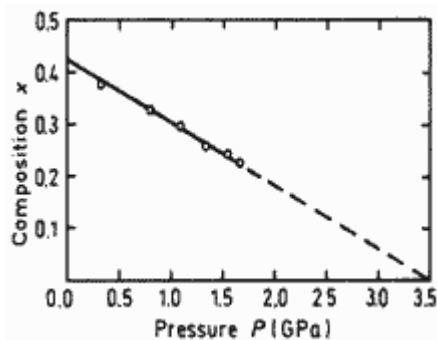
Dependences on Hydrostatic Pressure

$$E_c = (11.5 - 1.3x) \cdot 10^{-3} \cdot P \text{ (eV)}$$

$$E_X = -0.8 \cdot 10^{-3} \cdot P \text{ (eV)}$$

$$E_L = 2.8 \cdot 10^{-3} \cdot P \text{ (eV)}$$

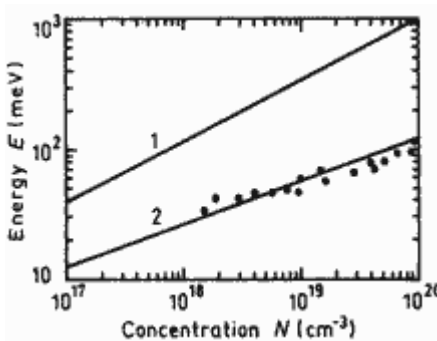
where P is pressure in kbar. ([Adachi \[1985\]](#))



Pressure dependence of the \bullet -X crossover. 300 K

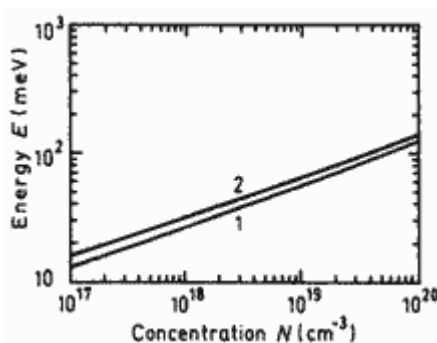
([Saxena \[1980\]](#))

Energy Gap Narrowing at High Doping Levels



Energy gap narrowing versus donor (curve 1) and acceptor (curve 2) doping density for GaAs ($x=0$).

Experimental points for p-GaAs are taken from four different papers ([Jain and Roulston \[1991\]](#))



Energy gap narrowing versus donor (curve 1) and acceptor (curve 2) doping density for AlAs ($x=1$).

The curves are calculated according ([Jain et al. \[1990\]](#))

Band Discontinuities at $\text{Al}_x\text{Ga}_{1-x}\text{As}/\text{GaAs}$ Heterointerface

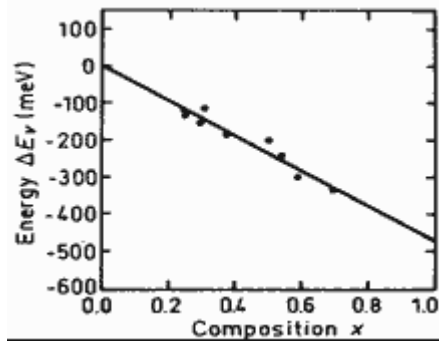
Valence band discontinuity:

- $E_v = -0.46x$ (eV)

Conduction band discontinuity:

- $x < 0.41$ • $E_c = 0.79x$ (eV)

- $x > 0.41$ • $E_c = 0.475 - 0.335x + 0.143x^2$ (eV)

**Energy gap narrowing versus donor (curve 1) and acceptor (curve 2) doping density for GaAs ($x=0$).**

Experimental points for p-GaAs are taken from four different papers
[\(Jain and Roulston \[1991\]\)](#)



Al_xGa_{1-x}As

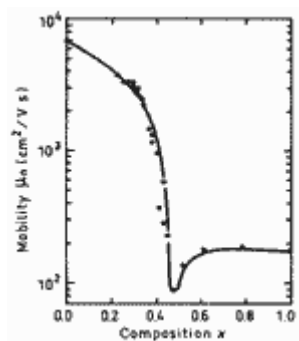
Electrical properties - Basic Parameters

Breakdown field	$\cdot(4\div 6) \cdot 10^5$ V/cm
Mobility electrons	
$0 < x < 0.45$	$8 \cdot 10^3 - 2.2 \cdot 10^4 x + 10^4 \cdot x^2$ cm ² V ⁻¹ s ⁻¹
$0.45 < x < 1$	$-255 + 1160x - 720x^2$ cm ² V ⁻¹ s ⁻¹
Mobility holes	$370 - 970x + 740x^2$ cm ² V ⁻¹ s ⁻¹
Diffusion coefficient electrons	
$0 < x < 0.45$	$200 - 550x + 250x^2$ cm ² /s
$0.45 < x < 1$	$-6.4 + 29x - 18x^2$ cm ² /s
Diffusion coefficient holes	$9.2 - 24x + 18.5x^2$ cm ² /s
Electron thermal velocity	
$0 < x < 0.4$	$(4.4 - 2.1x) \cdot 10^5$ m/s
$0.45 < x < 1$	$2.3 \cdot 10^5$ m/s
Hole thermal velocity	$(1.8 - 0.5x) \cdot 10^5$ m/s



Al_xGa_{1-x}As

Mobility and Hall Effect



Electron Hall mobility versus alloy composition x . $T=300$ K.

Electron concentration $n_0=(5\div 10)\cdot 10^{15}$ cm⁻³.

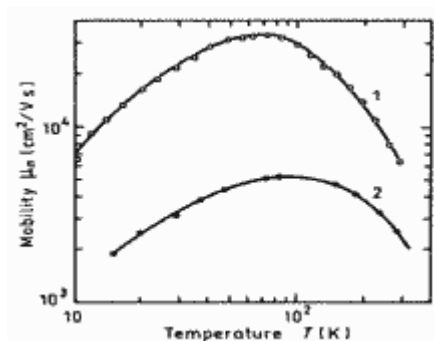
([Saxena \(1981b\)](#)).

For weakly doped Al_xGa_{1-x}As at 300 K electron Hall mobility.

$$0 < x < 0.45 \quad \mu_H = -8000 - 22000x + 10000x^2$$

$$0.45 < x < 1 \quad \mu_H = -255 + 1160x - 720x^2$$

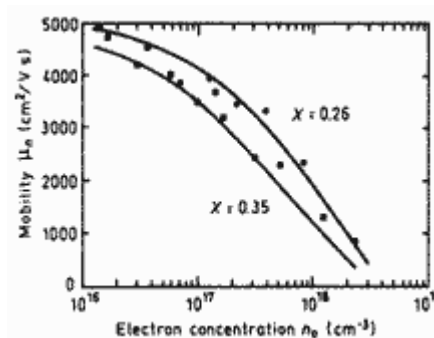
([Shur \(1990\)](#)).



Electron Hall mobility versus temperature.

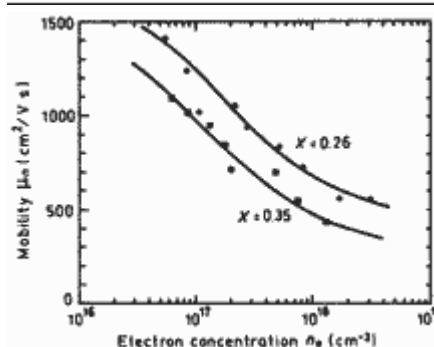
Curve 1 $x=0$; $n=0.5\cdot 10^{16}$ cm⁻³ ([Stillman et al. \(1970\)](#)).

Curve 2 $x=0.32$; $n=(0.5\div 1)\cdot 10^{16}$ cm⁻³ ([Saxena \(1981b\)](#)).



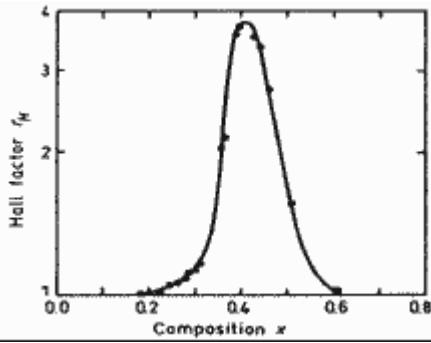
Electron Hall mobility versus electron concentration for two values of x . $T=77$ K.

([Liu \(1990\)](#)).



Electron Hall mobility versus electron concentration for two values of x . $T=300$ K.

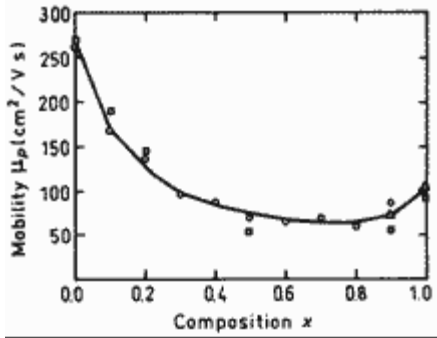
([Liu \(1990\)](#)).



Hall factor versus alloy composition x for n-type $Al_xGa_{1-x}As$ $T=300$ K

Electron concentration $n_0=(5\div 10)\cdot 10^{15} \text{ cm}^{-3}$.

[\(Saxena \(1981a\)\).](#)



Hole Hall mobility versus alloy composition x. 296 K.

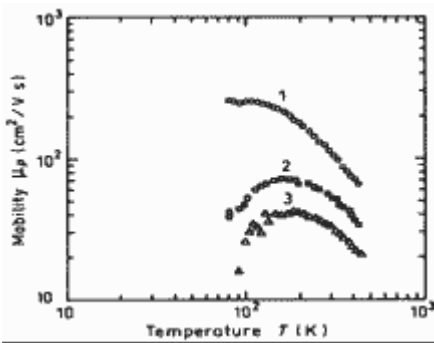
Acceptor density $N_a\cdot 2.5\cdot 10^{17} \text{ cm}^{-3}$.

[\(Look et al. \(1992\)\).](#)

For weakly doped $Al_xGa_{1-x}As$ at 300 K hole Hall mobility.

$$\mu_H = -370 - 970x + 740x^2$$

[\(Shur \(1990\)\).](#)



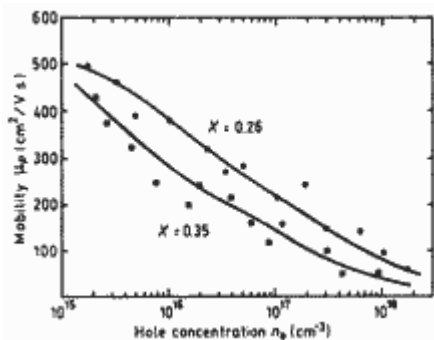
Hole Hall mobility versus temperature.

Curve 1 - $x=0$; $p_0=7\cdot 10^{17} \text{ cm}^{-3}$

Curve 2 - $x=0.41$; $p_0=4.65\cdot 10^{17} \text{ cm}^{-3}$

Curve 3 - $x=0.75$; $p_0=2.4\cdot 10^{17} \text{ cm}^{-3}$

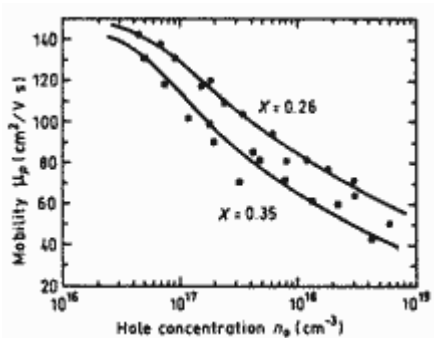
[\(Yang et al. \(1981\)\).](#)



Hole Hall mobility versus hole concentration for two values of x.

$T=77$ K.

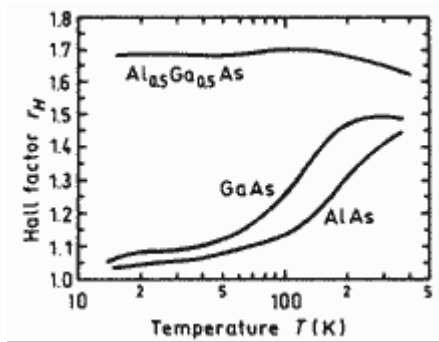
[\(Liu \(1990\)\).](#)



Hole Hall mobility versus hole concentration for two values of x.

$T=300$ K.

[\(Liu \(1990\)\).](#)



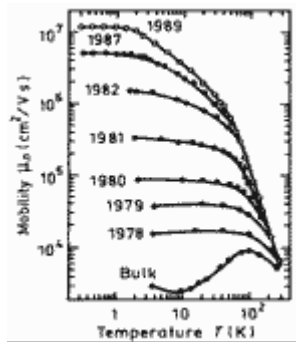
Hall factor versus temperature x for p-type GaAs, AlAs and $\text{Al}_{0.5}\text{Ga}_{0.5}\text{As}$.

Curves are calculated for acceptor concentration $N_a \cdot 6.5 \cdot 10^{13} \text{ cm}^{-3}$.
([Look et al. \(1992\)](#)).



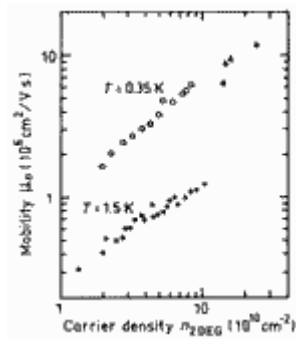
Al_xGa_{1-x}As

Two-dimensional electron and hole gas mobility at Al_xGa_{1-x}As/GaAs interface



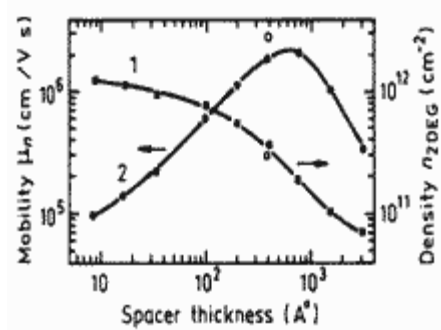
Temperature dependences of the electron Hall mobility in the modulation-doped two-dimensional gas.

([Pfeiffer et al. \(1989\)](#)).



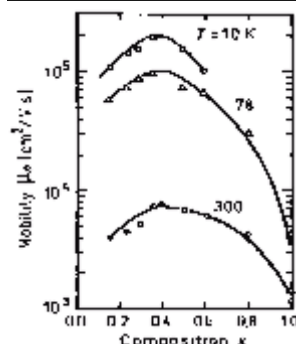
Dependences of electron mobility versus surface carrier density 2D electron gas in the modulation-doped two-dimensional gas.

([Pfeiffer et al. \(1989\)](#)).



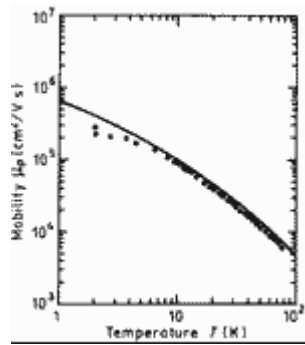
Dependences of surface electron density (Curve 1) and mobility (Curve 2) versus undoped spacer thickness. T=4 K.

([Harris et al. \(1987\)](#)).



Electron mobility in 2D-electron gas versus Al fraction x at three different temperatures.

([Drummond et al. \(1982\)](#)).

**Hole mobility in 2D-hole gas versus temperature.**

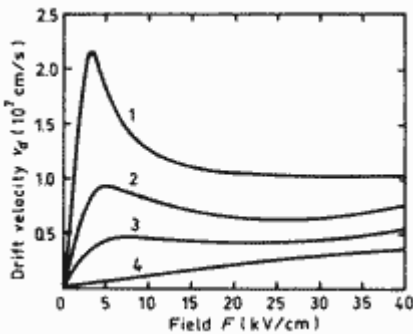
Solid line shows theoretical calculation.

Points show experimental data for hole surface density $2 \cdot 10^{11} \text{ cm}^{-2}$ ([Walukiewicz \(1996\)](#)).



Al_xGa_{1-x}As

Transport Properties in High Electric Fields

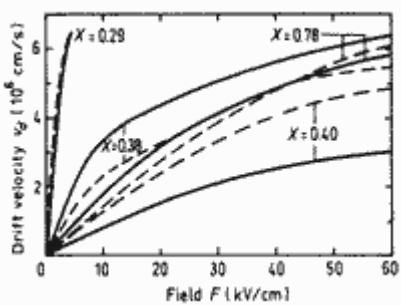


Field dependences of the electron drift velocity for different values of x .

Curves are calculated according displaced Maxwellian approximation.
 $T=300$ K.

- 1 - $x=0$;
- 2 - $x=0.225$;
- 3 - $x=0.325$;
- 4 - $x=0.5$.

[\(Hava and Auslender \(1993\)\).](#)

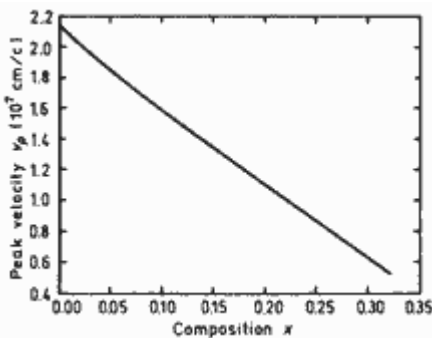


Field dependences of the electron drift velocity for different values of x .

Solid curves - show experimental results (electron concentration $n_0=(2\div 10)\cdot 10^{15}$ cm⁻³)

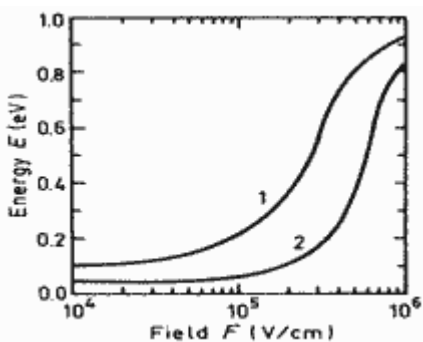
Dashed curves show results of Monte-Carlo calculations.

[\(Hill and Robson \(1981\)\).](#)



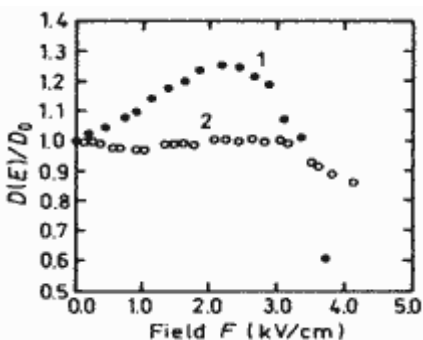
Dependences of peak electron velocity versus x .

[\(Hava and Auslender \(1993\)\).](#)



Average electron energy as a function of electric field. $T=300$ K.

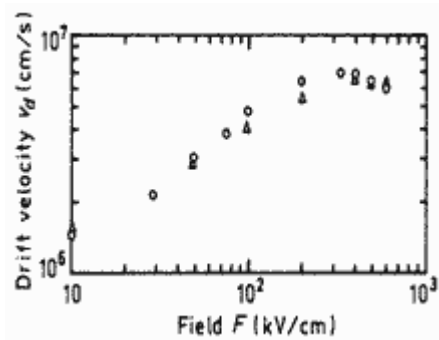
- 1 - $x=0.25$;
- 2 - $x=0.45$. [\(Lippens and Vanbesien \(1987\)\).](#)



The field dependences of normalized longitudinal diffusion coefficient.

$T=300$ K.

- 1 - $x=0$;
- 2 - $x=0.25$. [\(de Murcia et al. \(1993\)\).](#)



Field dependence of hole drift velocity. Monte-Carlo calculations.

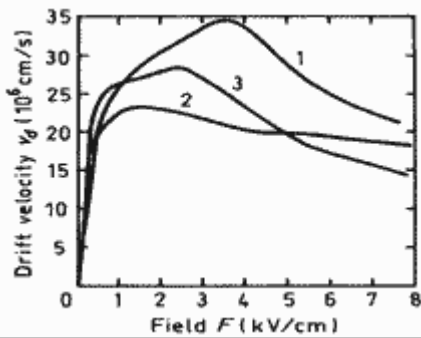
T=300 K.

(Brennan and Hess (1986)).



Al_xGa_{1-x}As

Transport properties of electron and hole two-dimensional gas in high electric field



Experimental field dependences of electron velocity.

T=77 K.

1 - for bulk GaAs with $n_0=10^{15} \text{ cm}^{-3}$

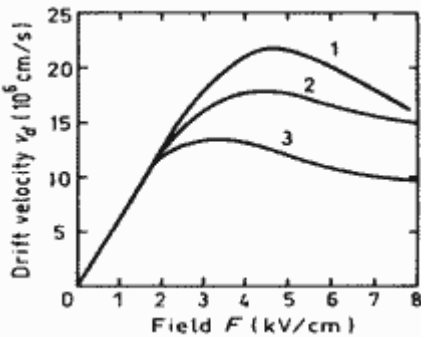
2, 3 - for two-dimensional modulation-doped heterostructures

Al_xGa_{1-x}As/GaAs.

2 - x=0.3;

3 - x=0.5.

[\(Masselink \(1989\)\).](#)



Experimental field dependences of electron velocity.

T=300 K.

1 - for bulk GaAs with $n_0=10^{15} \text{ cm}^{-3}$

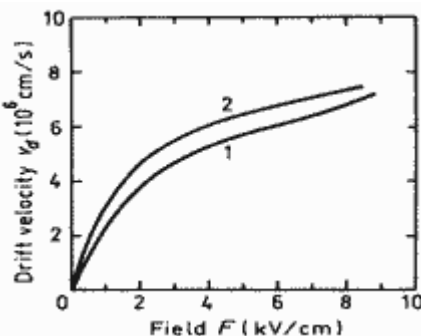
2, 3 - for two-dimensional modulation-doped heterostructures

Al_xGa_{1-x}As/GaAs.

2 - x=0.3;

3 - x=0.5.

[\(Masselink \(1989\)\).](#)



Experimental field dependences of hole velocity for two-dimensional hole gas. Single heterointerface samples. x=0.5. T=77 K.

1 - $p=3.3 \cdot 10^{11} \text{ cm}^{-2}$, $\mu=3300 \text{ cm}^2 \text{ Vs}$

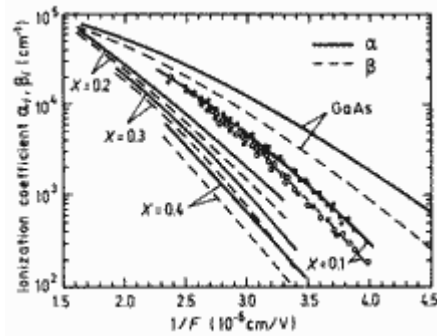
2 - $p=4.2 \cdot 10^{11} \text{ cm}^{-2}$, $\mu=4000 \text{ cm}^2 \text{ Vs}$

[\(Masselink et al. \(1987\)\).](#)



Al_xGa_{1-x}As

Impact Ionization



Fits to experimental values of electron and hole ionization coefficients for Al_xGa_{1-x}As with x=0.1÷0.4. T=300 K.

Experimental points are shown only for x=0.1 ([Robbins et al. \(1988\)](#)).

Parametrizations of the electron and hole ionization coefficients. T=300 K.

([Robbins et al.\(1988\)](#))

For electrons:

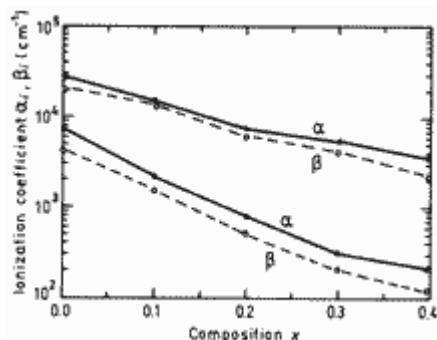
$$\alpha_i = \alpha_0 \exp\left[-\left(\frac{F_{no}}{F}\right)^m\right]$$

x	α_0 (cm ⁻¹)	F _{no} (V cm ⁻¹)	m
0.1	1.81•10 ⁵	6.31•10 ⁵	2.0
0.2	1.09•10 ⁶	1.37•10 ⁶	1.3
0.3	2.21•10 ⁵	7.64•10 ⁵	2.0
0.4	1.74•10 ⁷	3.39•10 ⁶	1.0

For holes:

$$\beta_i = \beta_0 \exp\left[-\left(\frac{F_{po}}{F}\right)^m\right]$$

x	β_0 (cm ⁻¹)	F _{po} (V cm ⁻¹)	m
0.1	3.05•10 ⁵	7.22•10 ⁵	1.9
0.2	6.45•10 ⁵	1.11•10 ⁶	1.5
0.3	2.791•10 ⁵	8.47•10 ⁵	1.9
0.4	3.06•10 ⁶	2.07•10 ⁶	1.2



Experimental ionization coefficients versus x for electric fields

Bottom curves - 3•10⁵ V/cm

Upper curves - 4•10⁵ V/cm

T=300 K. ([Robbins et al. \(1988\)](#)).

Breakdown voltage and breakdown field of n-GaAs/p-Al_{0.3}Ga_{0.7}As heterojunctions T=300 K.

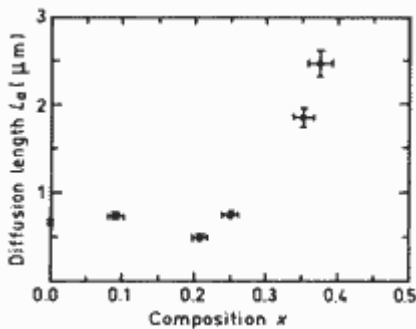
(Hur et al. (1990))

$N_a=10^{14} \text{ cm}^{-3}$	$V_i=2.8 \text{ kV}$	$E_i=2.8 \cdot 10^5 \text{ V cm}^{-1}$
$N_a=10^{16} \text{ cm}^{-3}$	$V_i=70 \text{ V}$	$E_i=4.5 \cdot 10^5 \text{ V cm}^{-1}$



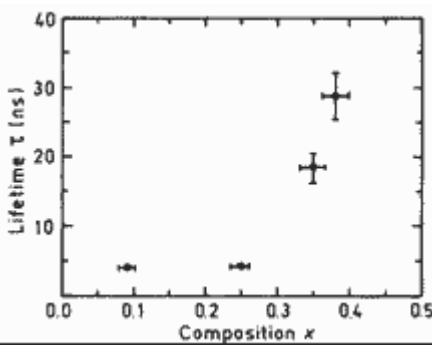
Al_xGa_{1-x}As

Recombination Parameter



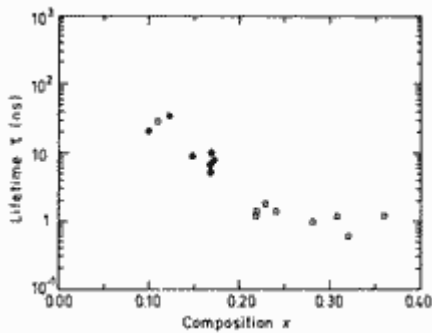
Ambipolar diffusion length at a carrier density of $10^{17} \div 10^{18} \text{ cm}^{-3}$ versus x . $T = 300\text{K}$.

Determination was accomplished by cathodoluminescence technique ([Zarem et al. \(1989\)](#)).



Carrier lifetimes at carrier density of $\sim 3 \cdot 10^{18} \text{ cm}^{-3}$ (high injection level) versus x . $T = 300\text{K}$.

Determination was accomplished by photoluminescence decay signal technique. ([Zarem et al. \(1989\)](#)).



Hole lifetime versus x for $n\text{-Al}_x\text{Ga}_{1-x}\text{As}$

$N_d - N_a \sim 10^{15} \div 10^{16} \text{ cm}^{-3}$. $T = 300\text{K}$.

([Timmons et al. \(1988\)](#)).

Radiative recombination coefficient at 300K $\sim 1.8 \cdot 10^{-10} \text{ cm}^3/\text{s}$

Auger coefficient at $T = 300 \text{ K}$ ([Timmons \(1985\)](#)).

x	$C_n \text{ (cm}^6/\text{s)}$	$C_p \text{ (cm}^6/\text{s)}$
0	$1.9 \cdot 10^{-31}$	$12 \cdot 10^{-31}$
0.1	$1.2 \cdot 10^{-31}$	$8.5 \cdot 10^{-31}$
0.2	$0.7 \cdot 10^{-31}$	$6.1 \cdot 10^{-31}$

C_n (for n -doped samples)

C_p (for p -doped samples)

Surface and interface recombination velocities in GaAs and $\text{Al}_x\text{Ga}_{1-x}\text{As}$

([Pavesi and Guzzi \(1994\)](#)).

x	S (cm/s)	
0	$4 \cdot 10^5$	free surface
0	45	interface between GaAs/Al _{0.3} Ga _{0.7} As
0	450±100	interface between GaAs/Al _{0.5} Ga _{0.5} As p-type
0.08	$4 \cdot 10^5$	free surface
0.08÷0.18	$\sim 3 \cdot 10^4$	interface between Al _x Ga _{1-x} As/Al _{0.88} Ga _{0.22} As undoped
0.28	4200	interface between Al _x Ga _{1-x} As/Al _{0.5} Ga _{0.5} As undoped

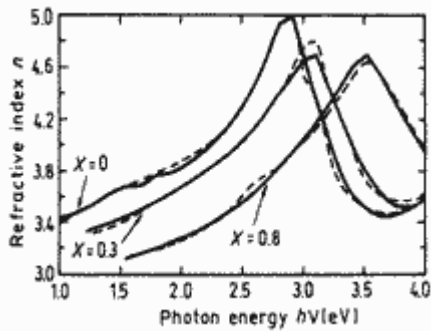


Al_xGa_{1-x}As

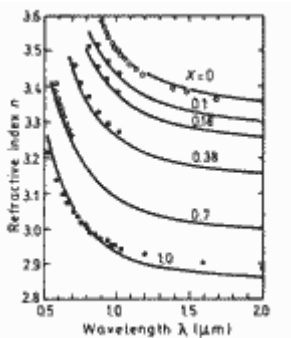
Optical properties

Infrared refractive index (300 K)

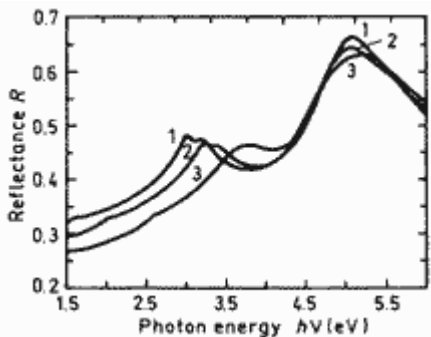
$$n = 3.3 - 0.53x + 0.09x^2$$



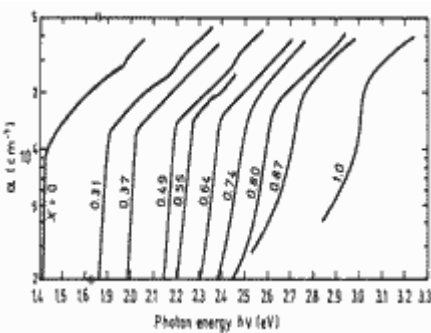
Refractive index n versus photon energy for three values of x .
Solid lines are calculated.
Dashed lines are experimental data. 300 K.
([Jenkins \(1990\)](#)).



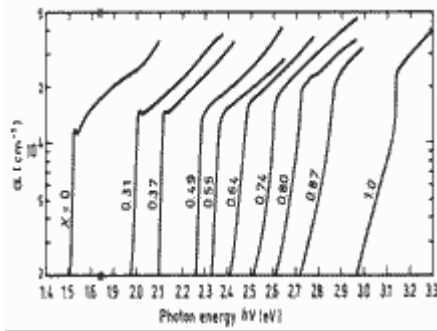
Refractive index n versus wavelength for different values of x . 300 K.
([Pikhtin and Yas'kov \(1980\)](#)).



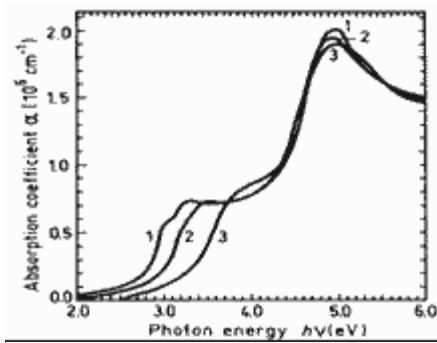
Normal incidence reflectivity versus photon energy. 300 K.
1 $x \sim 0.1$,
2 $x \sim 0.42$,
3 $x \sim 0.8$.
([Aspnes et al. \(1986\)](#))).



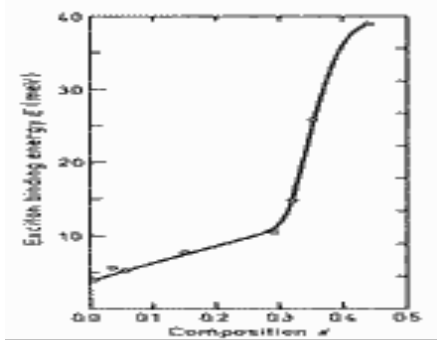
Intrinsic absorption coefficient near the intrinsic absorption edge for different values of x . 300 K.
([Monemar et al. \(1976\)](#)).



Intrinsic absorption coefficient near the intrinsic absorption edge for different values of x . 4 K.
 ([Monemar et al. \(1976\)](#)).



The absorption coefficient versus photon energy. 300 K.
 1 $x \sim 0.1$,
 2 $x \sim 0.42$,
 3 $x \sim 0.8$.
 ([Aspnes et al. \(1986\)](#)).



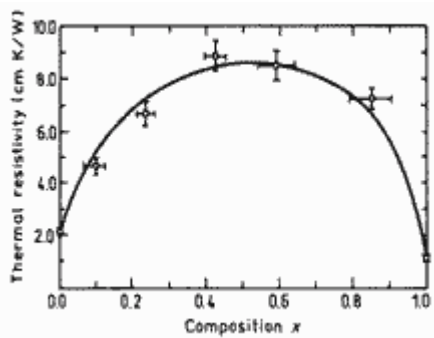
Free exciton binding energy versus Al mole fraction x .
 ([Pearah et al. \(1985\)](#)).



Al_xGa_{1-x}As

Thermal properties

Bulk modulus	$(7.55+0.26x) \cdot 10^{11} \text{ dyn cm}^{-2}$
Melting point	$1240-58x+558x^2 \text{ }^\circ\text{C}$ (<i>solidus curve</i>) $12401082x+582x^2 \text{ }^\circ\text{C}$ (<i>liquidus curve</i>)
Specific heat	$0.33+0.12x \text{ J g}^{-1}\text{ }^\circ\text{C}^{-1}$
Thermal conductivity	$0.55-2.12x+2.48x^2 \text{ W cm}^{-1} \text{ }^\circ\text{C}^{-1}$
Thermal diffusivity	$0.31-1.23x+1.46^2 \text{ cm}^2\text{s}^{-1}$
Thermal expansion, linear	$(5.73-0.53x) \cdot 10^{-6} \text{ }^\circ\text{C}^{-1}$



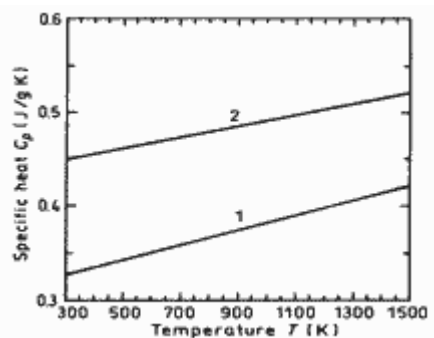
Thermal resistivity versus Al fraction x. 300K.

Solid curve is a theoretical fit to the experimental data.

([Afromowitz \[1973\]](#)).

Approximate formula for the lattice thermal resistivity:

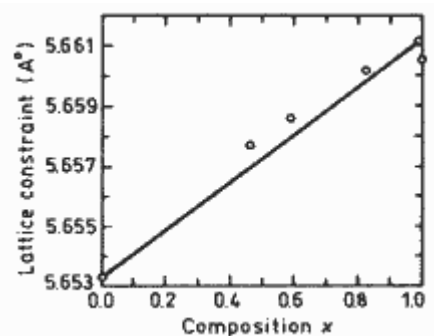
$$R_{\text{th}} = 2.27 + 28.83x - 30x^2 \text{ cm} \cdot \text{W}^{-1}$$



Temperature dependences of specific heat at constant pressure.

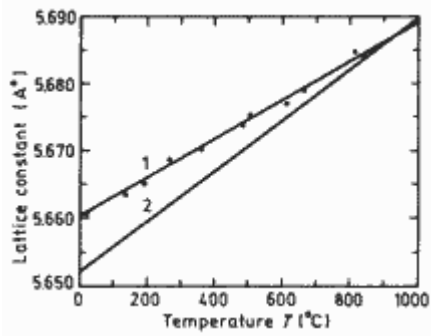
1. GaAs ([Lichter and Sommelet \[1969\]](#));

2. AlAs ([Barin et al. \[1977\]](#)).



Lattice constant as a function of x. 300K.

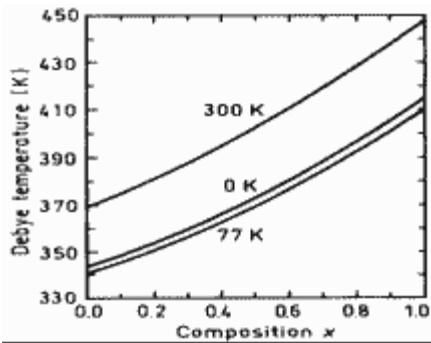
([Adachi \[1985\]](#)).



Lattice constants versus temperature.

1. AlAs;
2. GaAs;

([Ettenberg and Paff \[1970\]](#)).



Debye temperature as a function of x for three different temperatures.

([Adachi \[1985\]](#)).

Melting point:

$$T_m = 1240 - 58x + 558x^2 \text{ } ^\circ\text{C} \text{ (solidus curve)}$$

$$T_m = 1240 + 1082x - 582x^2 \text{ } ^\circ\text{C} \text{ (liquidus curve)}$$



Al_xGa_{1-x}As

Mechanical properties, elastic constants, lattice vibrations

[Basic Parameter](#)

[Elastic constants](#)

[Acoustic Wave Speeds](#)

[Phonon frequencies](#)

Basic Parameter

Bulk modulus	$(7.55+0.26x) \cdot 10^{11} \text{ dyn cm}^{-2}$
Density	$5.32-1.56x \text{ g cm}^{-3}$
Hardness on the Mohs scale	~ 5
Cleavage plane	{110}
Piezoelectric constant	$e_{14} = -0.16-0.065x \text{ C m}^{-2}$

Elastic constants 300 K.

$$C_{11} = (11.88 + 0.14x) \cdot 10^{11} \text{ dyn/cm}^2$$

$$C_{12} = (5.38 + 0.32x) \cdot 10^{11} \text{ dyn/cm}^2$$

$$C_{44} = (5.94 - 0.05x) \cdot 10^{11} \text{ dyn/cm}^2$$

[\(Adachi \[1985\]\)](#).

For T = 300 K

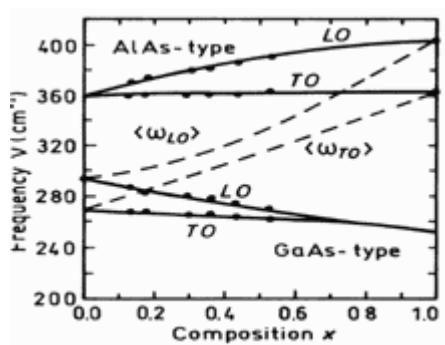
Bulk modulus (compressibility ⁻¹)	$B_s = (7.55 + 0.26x) \cdot 10^{11} \text{ dyn/cm}^2$
Anisotropy factor	$A = 0.55 - 0.01x$
Shear modulus	$C' = (3.25 - 0.09x) \cdot 10^{11} \text{ dyn/cm}^2$
[100] Young's modulus	$Y_0 = (8.53 - 0.18x) \cdot 10^{11} \text{ dyn/cm}^2$
[100] Poisson ratio	$\nu_0 = (0.31 + 0.1x)$

[\(Adachi \[1985\]\)](#).

Acoustic Wave Speeds

Wave propagation Direction	Wave character	Expression for wave speed	Wave speed (in units of 10^5 cm/s)
[100]	V_L	$(C_{11}/\rho)^{1/2}$	$4.73+0.68x+0.24x^2$
	V_T	$(C_{44}/\rho)^{1/2}$	$3.34+0.46x+0.16x^2$
[110]	V_I	$[(C_{11}+C_{12}+2C_{44})/2\rho]^{1/2}$	$5.24+0.78x+0.24x^2$
	$V_{t }$	$V_{t }=V_T=(C_{44}/\rho)^{1/2}$	$3.34+0.46x+0.16x^2$
	$V_{t\perp}$	$[(C_{11}-C_{12})/2\rho]^{1/2}$	$2.47+0.33x+0.10x^2$
[111]	V_I'	$[(C_{11}+2C_{12}+4C_{44})/3\rho]^{1/2}$	$5.40+0.79x+0.26x^2$
	V_t'	$[(C_{11}-C_{12}+C_{44})/3\rho]^{1/2}$	$2.79+0.38x+0.12x^2$

Phonon frequencies



Optical phonon energy as a function of x .

The compositional dependence of the effective phonon energy $\langle \omega_{LO} \rangle$ and $\langle \omega_{TO} \rangle$ are shown by the dashed lines.

([Adachi \[1985\]](#)).



Al_xGa_{1-x}As

References:

- Goldberg Yu.A. *Handbook Series on Semiconductor Parameters*, vol.2, M. Levinshtein, S. Rumyantsev and M. Shur, ed., World Scientific, London, 1999, pp. 1-36.

- S.Adachi, *J. Appl. Phys.*, **58**, no.3, pp.R1-R29 (1985).
- M.A.Afromowitz, *J. Appl. Phys.*, **44**, no.3, pp.1292-1294 (1973).
- D.E.Aspnes, *Phys. Rev.*, **B14**, no.12, pp.5331-5343 (1976).
- D.E.Aspnes, S.M.Kelso, R.A.Logan, R.Bhat., *J.Appl.Phys.*, **60**, no.2, pp.754-767 (1986).
- I. Barin, O. Knacke, O. Kubaschewski, *Thermochemical Properties of Inorganic Substances*, Springer, Berlin-Heidelberg-New York, 1977.
- K. Brennan, K. Hess, *J. Appl. Phys.*, **59**, no.3, pp.964-966 (1986).
- T. J. Drummond, W. Kopp, R. Fischer, H. Morkoc, *J. Appl. Phys.*, **53**, no.2, pp.1028-1029 (1982).
- M. Ettenberg, R. J. Paff, *J. Appl. Phys.*, **41**, no.10, pp.3926-3927 (1970).
- M.A. Haase, M.A. Emanuel, S.C. Smith, J.J. Coleman, and G.E. Stillman, *Appl. Phys. Lett.*, **50**, no.7, pp.404-406 (1987).
- J.J. Harris, C.T. Foxon, K.W.J. Barhkam, D.E. Lacklison, J. Hewett, C. White, *J. Appl. Phys.*, **61**, no.3, pp.1219-1221 (1987)
- S. Hava, M. Auslender, *J. Appl. Phys.*, **73**, no.11, pp.7431-7434 (1993).
- R. Heilman, G. Oelgart, *Semicond. Sci. Technol.*, **5**, no 10, pp.1040-1045 (1990).
- G. Hill, and P.N.Robson, *J.de Physique*, **42**, Colloque no.7, Suppl. au no.10, pp.C7-335 - C7-341 (1981).
- J.H. Hur, C.W. Myles, M.A. Gundersen, *J. Appl. Phys.*, **67**, no.11, pp.6917-6923 (1990).
- S.C.Jain, J.M.McGregor, D.J.Roulston, *J. Appl. Phys.*, **68**, no.7, pp.3747-3749 (1990).
- S.C.Jain, and D.J.Roulston, *Solid State Electron*, **34**, no.5, pp.453-465 (1991).
- D.W.Jenkins, *J. Appl. Phys.*, **68**, no.4, pp.1848-1853 (1990).
- K.Kaneko, M.Ayabe, and N.Watanabe, in *GaAs and Related Compounds* (Inst.of Phys., London, Ser . 33a, 1977), pp.216-226.
- J.M.Langer, H.Heinrich, *Physica B*, **134** no.1-3, pp.444-450 (1985).
- B.D.Lichter and P.Sommelet, *Trans. Metall. Soc., AIME*, **245**, pp.1021-1027 (1969).
- D.Lippens, O.Vanbesien, in *GaAs and Related Compounds* (Inst.of Phys., Bristol and Philadelphia, Ser. 91, 1987), pp.757-760.
- W.C.Liu, *J. Material Sci.*, **25**, no.3, pp.1765-1772 (1990).
- D.C.Look, D.K.Lorance, J.R.Sizelove, C.E.Stutz, K.R.Evans, D.W.Whitson, *J. Appl. Phys.*, **71**, no.1, pp.260-266 (1992).
- W.T.Masselink, *Semicond. Sci. Technol.*, **4**, no.7, pp.503-512 (1989).
- W.T.Masselink,N.Braslau, D.LaTulipe, W.I.Wang, S.L.Wright, in *GaAs and Related Compounds* (Inst. of Phys.,Bristol and Philadelphia, Ser. 91, 1987), pp.665-668.
- B.Monemar, K.K. Shih, and G.D.Pettit, *J. Appl. Phys.*, **47**, no.6, pp.2604-2613 (1976).
- M.de Murcia, D.Gasquet, E.Richard, P.Wolff, J.Zimmermann, J.Vanbremeersch, *AIP Conf. Proc.* 285 (Noise in Physical Systems and 1/f fluctuations, St.Louis, USA, 1993), pp.27-30 .
- L. Pavesi, M.Guzzi, *J. Appl. Phys.*, **75**, no.10, pp.4779-4842 (1994).
- P.J.Pearah, W.T.Masselink, J.Klem, T.Henderson, H.Morcoc, C.W.Litton, D.C.Reynolds, *Phys.Rev.*, **B32**, no.6, pp.3857-3862 (1985).
- L.Pfeiffer, K.W.West, H.L.Stormer, K.W.Baldwin, *Appl. Phys. Lett.*, **55**, no.18, pp.1888-1890 (1989).
- A.N.Pikhtin, A.D.Yas'kov, *Sov.Phys.Semicond.*, **14**, no.4, pp.389-392 (1980).
- V.M.Robbins, S.C.Smith, G.E.Stillman, *Appl. Phys. Lett*, **52**, no.4, pp.296-298 (1988).
- A.K. Saxena, *J. Phys. C.*, **13**, no.23, pp. 4323-4334 (1980).
- A. K. Saxena, *Solid St. Comm.*, **39**, no.7, pp. 839-842 (1981).
- A.K.Saxena, *Phys. Rev.*, **B24**, no.6, pp. 3295-3302 (1981).
- M.Shur, *Physics of Semiconductor Devices*, Prentice Hall, 1990.
- A.J. Spring Thorpe, T.D. King, A.J. Beck, *J. Electron. Mater.*, **4**, no.1, pp. 101-118 (1975).
- G.E.Stillman, C.M. Wolfe, and J.O. Dimmock, *J. Phys. Chem. Solids*, **31**, no. 6, pp. 1199-1204 (1970).

- M.Takeshima, *J. Appl. Phys.*, **58**, no.10, p.3846 (1985)
- M.L. Timmons, J.A. Hutchby, R.K. Ahrenkiel, D.J. Dunlavy, in *GaAs and Related Compounds* (Inst. of Phys., Bristol and Philadelphia, Ser. 96, 1988), pp. 289-294.
- W.Walukiewicz, *J. Appl. Phys.*, **59**, no.10, pp.3577-3579 (1986).
- Z.Wilamowski, J.Kossut, W.Jantsch, and G.Ostermayer, *Semicond.Sci.Technol.*, **6**, no.10B, pp.B38-B46 (1991).
- J.J.Yang, W.I.Simpson, L.A.Moudy, in *GaAs and Related Compounds* (Inst. of Phys., Bristol and London, Ser.63, 1981), pp.107-112.
- J.J.Yang, L.A.Moudy, W.I.Simpson, *Appl. Phys. Lett.*, **40**, no. 3, pp.244-246 (1982).
- H.A.Zarem, J.A.Lebens, K.B.Nordstrom, P.C.Sercel, S.Sanders, L.E.Eng, A.Yariv, K.J.Vahala, *Appl.Phys.Lett.*, **55**, no. 25, pp.2622-2624 (1989).



GaAs - Gallium Arsenide

- [Basic Parameters at 300 K](#)
- [Band structure and carrier concentration](#)
 - [Basic Parameters of Band Structure and carrier concentration](#)
 - [Temperature Dependences](#)
 - [Energy Gap Narrowing at High Doping Levels](#)
 - [Effective Masses and Density of States](#)
 - [Donors and Acceptors](#)
- [Electrical Properties](#)
 - [Basic Parameters of Electrical Properties](#)
 - [Mobility and Hall Effect](#)
 - [Transport Properties in High Electric Fields](#)
 - [Impact Ionization](#)
 - [Recombination Parameters](#)
- [Optical properties](#)
- [Thermal properties](#)
- [Mechanical properties, elastic constants, lattice vibrations](#)
 - [Basic Parameters](#)
 - [Elastic Constants](#)
 - [Acoustic Wave Speeds](#)
 - [Phonon Frequencies](#)
- [References](#)



GaAs - Gallium Arsenide

Basic Parameters at 300 K

Crystal structure	Zinc Blende
Group of symmetry	T_d^2-F43m
Number of atoms in 1 cm^3	$4.42 \cdot 10^{22}$
de Broglie electron wavelength	240 Å
Debye temperature	360 K
Density	5.32 g cm^{-3}
Dielectric constant (static)	12.9
Dielectric constant (high frequency)	10.89
Effective electron mass m_e	$0.063m_0$
Effective hole masses m_h	$0.51m_0$
Effective hole masses m_{lp}	$0.082m_0$
Electron affinity	4.07 eV
Lattice constant	5.65325 Å
Optical phonon energy	0.035 eV



GaAs - Gallium Arsenide

Band structure and carrier concentration

[Basic Parameters](#)

[Temperature Dependences](#)

[Dependence of the Energy Gap on Hydrostatic Pressure](#)

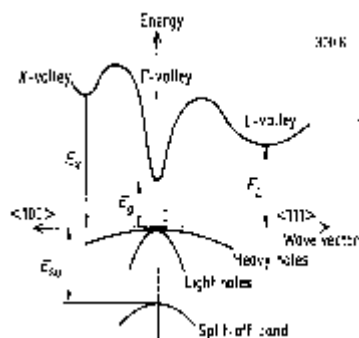
[Energy Gap Narrowing at High Doping Levels](#)

[Effective Masses](#)

[Donors and Acceptors](#)

Basic Parameters

Energy gap	1.424 eV
Energy separation ($E_{\bullet-L}$) between \bullet and L valleys	0.29 eV
Energy separation ($E_{\bullet-X}$) between \bullet and X valleys	0.48 eV
Energy spin-orbital splitting	0.34 eV
Intrinsic carrier concentration	$2.1 \cdot 10^6 \text{ cm}^{-3}$
Intrinsic resistivity	$3.3 \cdot 10^8 \text{ } \Omega \cdot \text{cm}$
Effective conduction band density of states	$4.7 \cdot 10^{17} \text{ cm}^{-3}$
Effective valence band density of states	$9.0 \cdot 10^{18} \text{ cm}^{-3}$



Band structure and carrier concentration of GaAs. 300 K

$E_g = 1.42 \text{ eV}$
$E_L = 1.71 \text{ eV}$
$E_X = 1.90 \text{ eV}$
$E_{SO} = 0.34 \text{ eV}$

Temperature Dependences

Temperature dependence of the energy gap

$$E_g = 1.519 - 5.405 \cdot 10^{-4} \cdot T^2 / (T + 204) \text{ (eV)}$$

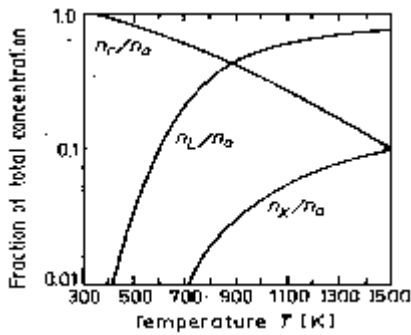
where T is temperatures in degrees K ($0 < T < 10^3$).

Temperature dependence of the energy difference between the top of the valence band and the bottom of the L-valley of the conduction band

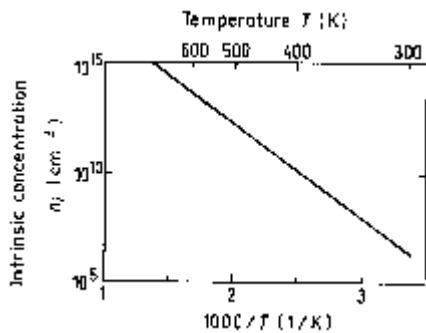
$$E_L = 1.815 - 6.05 \cdot 10^{-4} \cdot T^2 / (T + 204) \text{ (eV)}$$

Temperature dependence of the energy difference between the top of the valence band and the bottom of the X-valley of the conduction band

$$E_L = 1.981 - 4.60 \cdot 10^{-4} \cdot T^2 / (T + 204) \text{ (eV)}$$



The temperature dependences of the relative populations of the Γ , L and X valleys. ([Blakemore \[1982\]](#)).



The temperature dependences of the intrinsic carrier concentration. ([Shur \[1990\]](#)).

Intrinsic Carrier Concentration

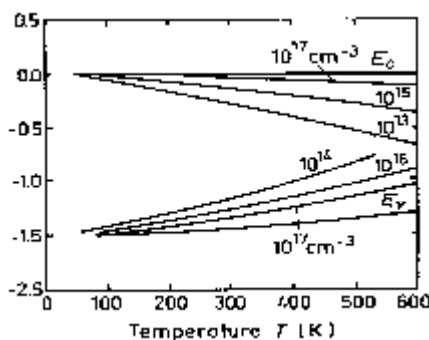
$$n_i = (N_c \cdot N_v)^{1/2} \exp(-E_g / (2k_b T))$$

Effective density of states in the conduction band taking into account the nonparabolicity of the Γ -valley and contributions from the X and L-valleys

$$N_c = 8.63 \cdot 10^{13} \cdot T^{3/2} [1 - 1.9310^{-4} \cdot T - 4.19 \cdot 10^{-8} \cdot T^2 + 21 \cdot \exp(-E_L / (2k_b T)) + 44 \cdot \exp(-E_X / (2k_b T))] \text{ (cm}^{-3}\text{)}$$

Effective density of states in the valence band

$$N_v = 1.83 \cdot 10^{15} \cdot T^{3/2} \text{ (cm}^{-3}\text{)}$$



Fermi level versus temperature for different concentrations of shallow donors and acceptors.

Dependences on Hydrostatic Pressure

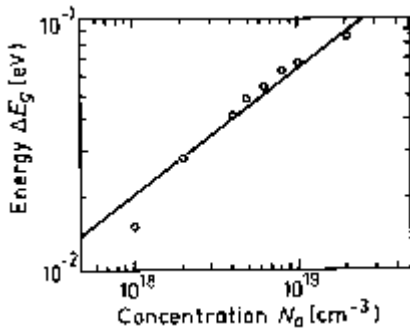
$$E_g = E_g(0) + 0.0126 \cdot P - 3.77 \cdot 10^{-5} P^2 \text{ (eV)}$$

$$E_L = E_L(0) + 5.5 \cdot 10^{-3} P \text{ (eV)}$$

$$E_X = E_X(0) + 1.5 \cdot 10^{-3} P \text{ (eV)}$$

where P is pressure in kbar.

Energy Gap Narrowing at High Doping Levels



Energy gap narrowing at high doping levels.
([Tiwari and Wright \[1990\]](#))

$$\bullet E_g \bullet 2 \cdot 10^{-11} \bullet N_a^{-1/2} \text{ (eV) } (N_a \text{ in cm.}^{-3})$$

Effective Masses

Electrons:

For \bullet -valley $m_{\bullet} = 0.063m_0$

In the L-valley the surfaces of equal energy are ellipsoids

$$m_l = 1.9m_0$$

$$m_t = 0.075m_0$$

Effective mass of density of states

$$m_L = (16m_l m_t^2)^{1/3} \quad m_L = 0.85m_0$$

In the X-valley the surfaces of equal energy are ellipsoids

$$m_l = 1.9m_0$$

$$m_t = 0.19m_0$$

Effective mass of density of states

$$m_X = (9m_l m_t^2)^{1/3} \quad m_X = 0.85m_0$$

Holes:

Heavy $m_h = 0.51m_0$

Light $m_{lp} = 0.082m_0$

Split-off band $m_{so} = 0.15m_0$

Effective mass of density of states $m_v = 0.53m_0$

Donors and Acceptors

Ionization energies of shallow donors (eV)

([Milnes \[1973\]](#))

S	Se	Si	Ge	Sn	Te
~0.006	~0.006	~0.006	~0.006	~0.006	~0.03

Ionization energies of shallow acceptors (eV)

([Milnes \[1973\]](#))

C	Si	Ge	Zn	Sn
-0.02	~0.03/0.1/0.22	~0.03	~0.025	~0.2



GaAs - Gallium Arsenide

Electrical properties

[Basic Parameters](#)

[Mobility and Hall Effect](#)

[Transport Properties in High Electric Fields](#)

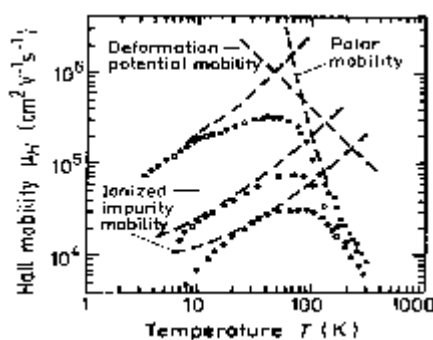
[Impact Ionization](#)

[Recombination Parameters](#)

Basic Parameters

Breakdown field	$\bullet 4 \cdot 10^5$ V/cm
Mobility electrons	$\bullet 8500$ cm ² V ⁻¹ s ⁻¹
Mobility holes	$\bullet 400$ cm ² V ⁻¹ s ⁻¹
Diffusion coefficient electrons	$\bullet 200$ cm ² /s
Diffusion coefficient holes	$\bullet 10$ cm ² /s
Electron thermal velocity	$4.4 \cdot 10^5$ m/s
Hole thermal velocity	$1.8 \cdot 10^5$ m/s

Mobility and Hall Effect



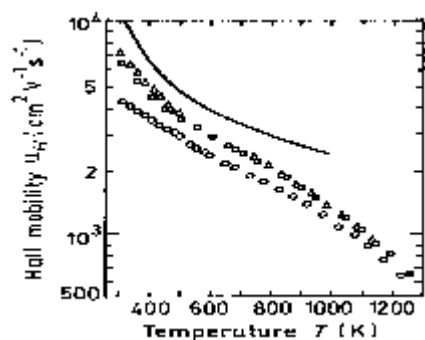
Electron Hall mobility versus temperature for different doping levels.

[\(Stillman et al. \[1970\]\)](#)

1. Bottom curve: $N_d = 5 \cdot 10^{15}$ cm⁻³;
2. Middle curve: $N_d = 10^{15}$ cm⁻³;
3. Top curve: $N_d = 5 \cdot 10^{15}$ cm⁻³

For weakly doped GaAs at temperature close to 300 K, electron Hall mobility

$$\mu_H = 9400(300/T) \text{ cm}^2 \text{ V}^{-1} \text{ s}^{-1}$$



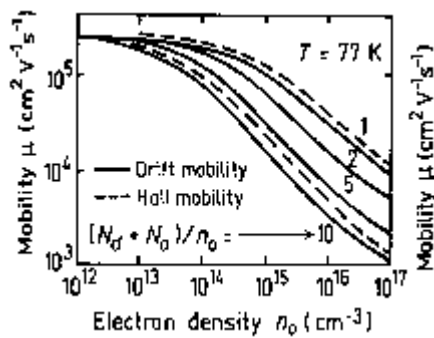
Electron Hall mobility versus temperature for different doping levels and degrees of compensation (high temperatures):

- Open circles: $N_d = 4N_a = 1.2 \cdot 10^{17}$ cm⁻³;
- Open squares: $N_d = 4N_a = 10^{16}$ cm⁻³;
- Open triangles: $N_d = 3N_a = 2 \cdot 10^{15}$ cm⁻³;

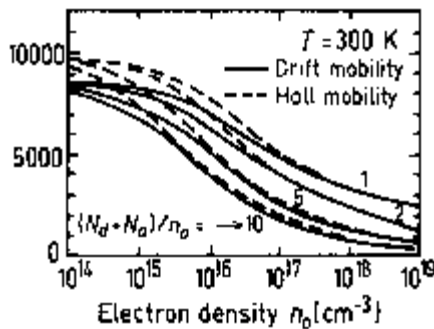
Solid curve represents the calculation for pure GaAs [\(Blakemore \[1982\]\)](#).

For weakly doped GaAs at temperature close to 300 K, electron drift mobility

$$\mu_n = 8000(300/T)^{2/3} \text{ cm}^2 \text{ V}^{-1} \text{ s}^{-1}$$



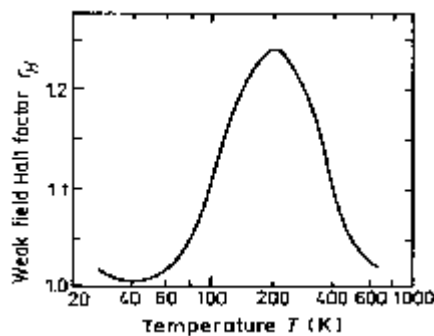
Drift and Hall mobility versus electron concentration for different degrees of compensation $T = 77$ K
(Rode [1975]).



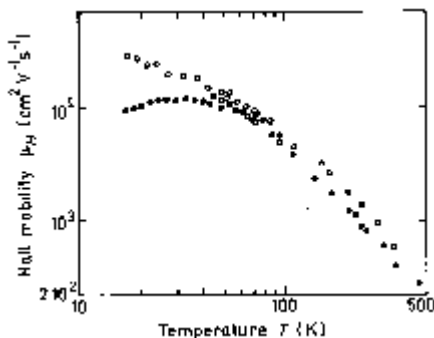
Drift and Hall mobility versus electron concentration for different degrees of compensation $T = 300$ K
(Rode [1975]).

Approximate formula for the Hall mobility

$\mu_n = \mu_{OH} / (1 + N_d \cdot 10^{-17})^{1/2}$, where $\mu_{OH} \approx 9400$ ($\text{cm}^2 \text{V}^{-1} \text{s}^{-1}$), N_d in cm^{-3}
(Hilsum [1974]).



Temperature dependence of the Hall factor for pure n -type GaAs in a weak magnetic field
(Rode [1975]).



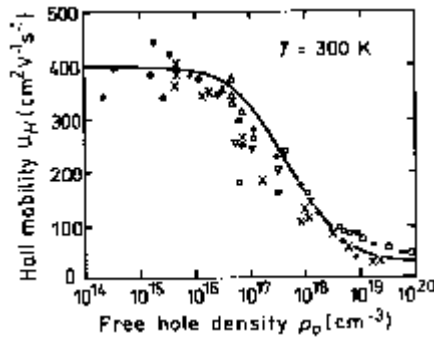
Temperature dependence of the Hall mobility for three high-purity samples
(Wiley [1975]).

For GaAs at temperatures close to 300 K, hole Hall mobility

$$\mu_{pH} = \left[0.0025 \left(\frac{T}{300} \right)^{2.3} + 4 \times 10^{21} p \left(\frac{T}{300} \right)^{1.5} \right]^{-1} \quad (\text{cm}^2 \text{V}^{-1} \text{s}^{-1}), \quad (p - \text{in } \text{cm}^{-3})$$

For weakly doped GaAs at temperature close to 300 K, Hall mobility

$$\mu_{pH} = 400 (300/T)^{2.3} \quad (\text{cm}^2 \text{V}^{-1} \text{s}^{-1}).$$



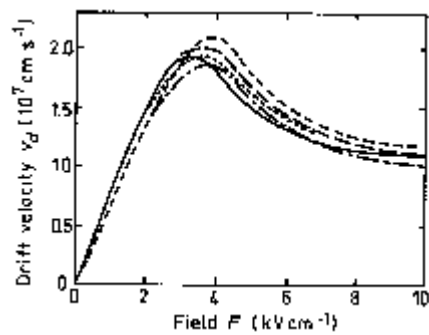
The hole Hall mobility versus hole density.

([Wiley \[1975\]](#))

At $T = 300\text{ K}$, the Hall factor in pure GaAs

$$r_H = 1.25.$$

Transport Properties in High Electric Fields

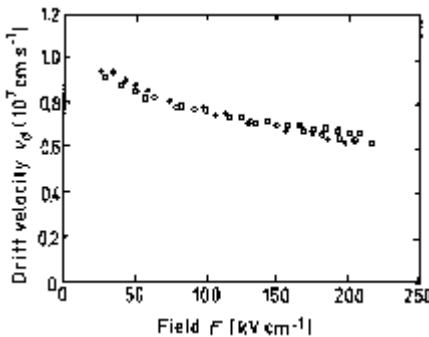


Field dependences of the electron drift velocity.

([Blakemore \[1982\]](#)).

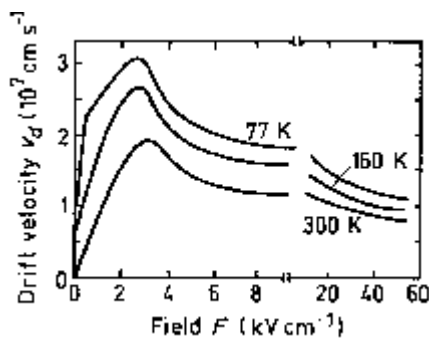
Solid curve was calculated by ([Pozhela and Reklaitis \[1980\]](#)).

Dashed and dotted curves are measured data, 300 K



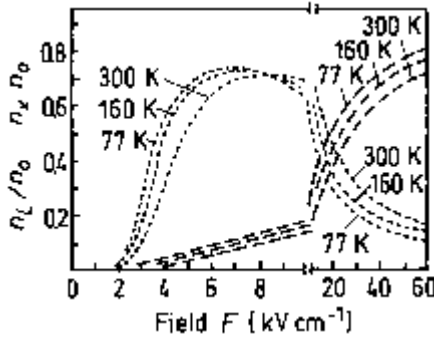
Field dependences of the electron drift velocity for high electric fields, 300 K .

([Blakemore \[1982\]](#)).

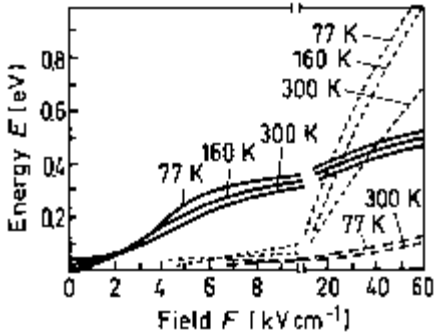


Field dependences of the electron drift velocity at different temperatures.

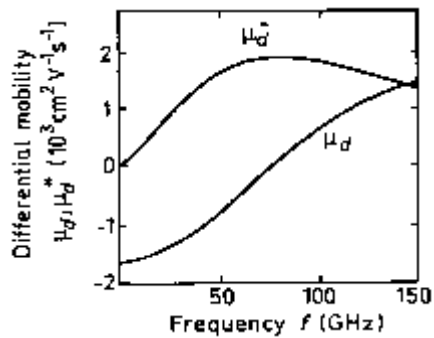
([Pozhela and Reklaitis \[1980\]](#)).



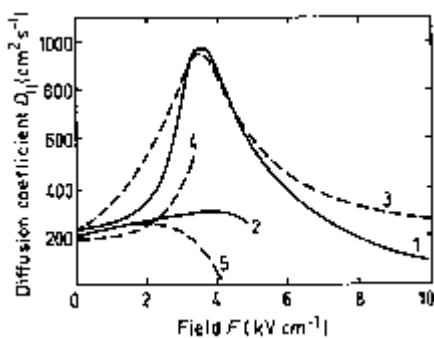
Fraction of electrons in L and X valleys. n_L and n_X as a function of electric field F at 77, 160, and 300 K, $N_d=0$
 ([Pozhela and Reklaitis\[1980\]](#)).
 Dotted curve - L valleys, dashed curve - X valleys.



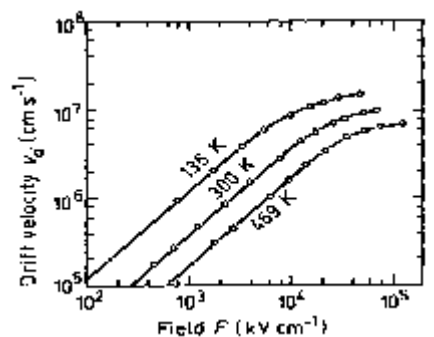
Mean energy E in \bullet , L , and X valleys as a function of electric field F at 77, 160, and 300 K, $N_d=0$
 ([Pozhela and Reklaitis\[1980\]](#)).
 Solid curve - \bullet valleys, dotted curve - L valleys, dashed curve - X valleys.



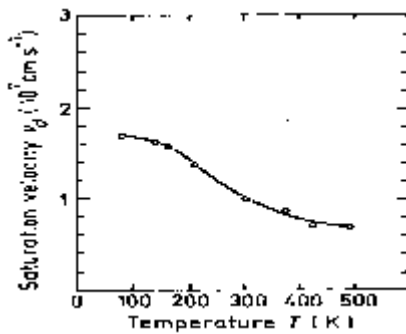
Frequency dependences of electron differential mobility.
 μ_d is real part of the differential mobility; μ_d^* is imaginary part of differential mobility.
 $F=5.5 \text{ kV cm}^{-1}$
 ([Rees\[1969\]](#)).



The field dependence of longitudinal electron diffusion coefficient $D_{||}F$.
 Solid curves 1 and 2 are theoretical calculations. Dashed curves 3, 4, and 5 are experimental data.
 Curve 1 - from ([Pozhela and Reklaitis\[1980\]](#)).
 Curve 2 - from ([Fauquembergue et al.\[1980\]](#)).
 Curve 3 - from ([Ruch and Kino\[1968\]](#)).
 Curve 4 - from ([Bareikis et al.\[1978\]](#)).
 Curve 5 - ([from de Murcia\[1991\]](#)).

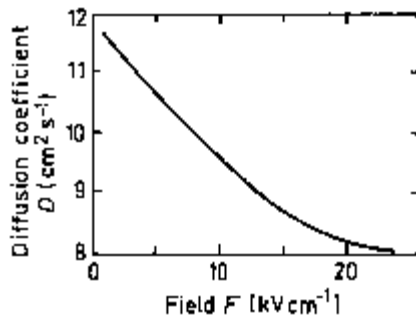


Field dependences of the hole drift velocity at different temperatures.
 ([Datal et al. \[1971\]](#)).



Temperature dependence of the saturation hole velocity in high electric fields

([Datal et al. \[1971\]](#)).



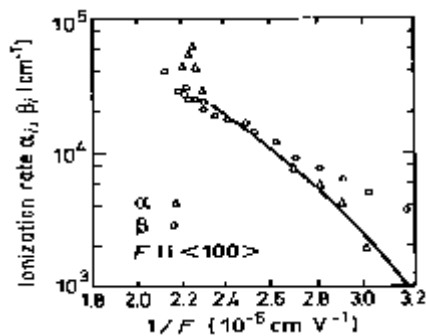
The field dependence of the hole diffusion coefficient.

([Joshi and Crendin \[1989\]](#)).

Impact Ionization

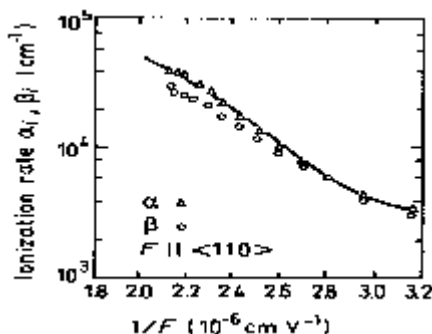
There are two schools of thought regarding the impact ionization in GaAs.

The first one states that impact ionization rates α_i and β_i for electrons and holes in GaAs are known accurately enough to distinguish such subtle details such as the anisotropy of α_i and β_i for different crystallographic directions. This approach is described in detail in the work by Dmitriev et al. [1987].



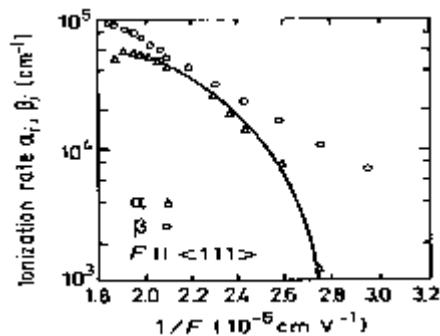
Experimental curves α_i and β_i versus $1/F$ for GaAs.

([Pearsall et al. \[1978\]](#)).



Experimental curves α_i and β_i versus $1/F$ for GaAs.

([Pearsall et al. \[1978\]](#)).



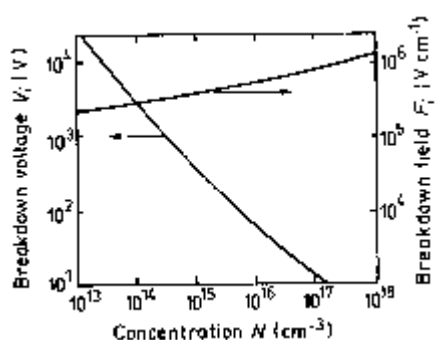
Experimental curves α_i and β_i versus $1/F$ for GaAs.

(Pearsall et al. [1978]).

The second school focuses on the values of α_i and β_i for the same electric field reported by different researches differ by an order of magnitude or more. This point of view is explained by Kyuregyan and Yurkov [1989]. According to this approach we can assume that $\alpha_i = \beta_i$. Approximate formula for the field dependence of ionization rates:

$$\alpha_i = \beta_i = \alpha_0 \exp[\alpha_0^2 + (F_0/F)^2]^{1/2}$$

where $\alpha_0 = 0.245 \cdot 10^6 \text{ cm}^{-1}$; $F_0 = 57.6 F_0 = 6.65 \cdot 10^6 \text{ V cm}^{-1}$ (Kyuregyan and Yurkov [1989]).



Breakdown voltage and breakdown field versus doping density for an abrupt $p-n$ junction.

(Kyuregyan and Yurkov [1989]).

Recombination Parameter

Pure n-type material ($n_0 \sim 10^{14} \text{ cm}^{-3}$)

The longest lifetime of holes $\tau_p \sim 3 \cdot 10^{-6} \text{ s}$

Diffusion length $L_p = (D_p \tau_p)^{1/2}$ $L_p \sim 30\text{-}50 \text{ }\mu\text{m}$.

Pure p-type material

(a) Low injection level

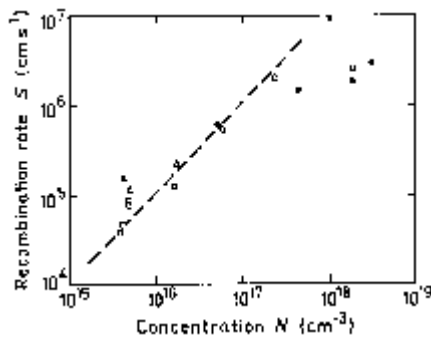
The longest lifetime of electrons $\tau_n \sim 5 \cdot 10^{-9} \text{ s}$

Diffusion length $L_n = (D_n \tau_n)^{1/2}$ $L_n \sim 10 \text{ }\mu\text{m}$

(b) High injection level (filled traps)

The longest lifetime of electrons $\tau_n \sim 2.5 \cdot 10^{-7} \text{ s}$

Diffusion length L_n $L_n \sim 70 \text{ }\mu\text{m}$



Surface recombination velocity versus doping density

([Aspnes \[1983\]](#)).

Different experimental points correspond to different surface treatment methods.

Radiative recombination coefficient ([Varshni\[1967\]](#))

$$90 \text{ K } 1.8 \cdot 10^{-8} \text{ cm}^3/\text{s}$$

$$185 \text{ K } 1.9 \cdot 10^{-9} \text{ cm}^3/\text{s}$$

$$300 \text{ K } 7.2 \cdot 10^{-10} \text{ cm}^3/\text{s}$$

Auger coefficient

$$300 \text{ K } \sim 10^{-30} \text{ cm}^6/\text{s}$$

$$500 \text{ K } \sim 10^{-29} \text{ cm}^6/\text{s}$$



GaAs - Gallium Arsenide

Optical properties

Infrared refractive index 3.3
 Radiative recombination coefficient $7 \cdot 10^{-10} \text{ cm}^3/\text{s}$

Infrared refractive index

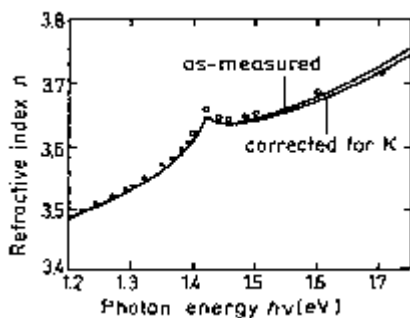
$n = k^{1/2} = 3.255 \cdot (1 + 4.5 \cdot 10^{-5} T)$
 for 300 K $n = 3.299$

Long-wave *TO* phonon energy

$h \cdot \omega_{TO} = 33.81 \cdot (1 - 5.5 \cdot 10^{-5} T)$ (meV)
 for 300 K $h \cdot \omega_{TO} = 33.2$ meV

Long-wave *LO* phonon energy

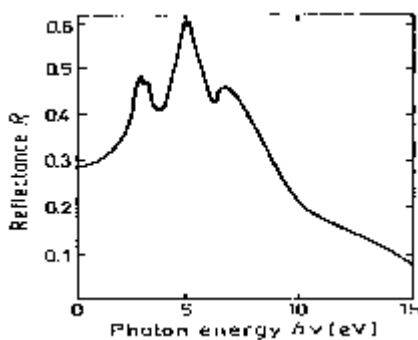
$h \cdot \omega_{LO} = 36.57 \cdot (1 - 4 \cdot 10^{-5} T)$ (meV)
 for 300 K $h \cdot \omega_{LO} = 36.1$ meV



Refractive index n versus photon energy for a high-purity

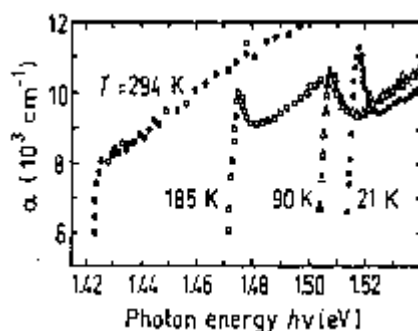
GaAs. ($n_0 \sim 5 \cdot 10^{13} \text{ cm}^{-3}$).

Solid curve is deduced from two-beam reflectance measurements at 279 K. Dark circles are obtained from refraction measurements. Light circles are calculated from Kramers-Kronig analysis ([Blakemore \[1982\]](#)).



Normal incidence reflectivity versus photon energy.

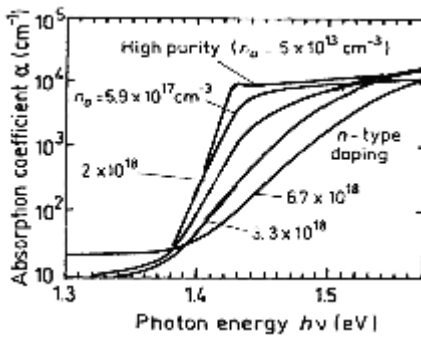
([Phillip and Ehrenreich \[1963\]](#)).



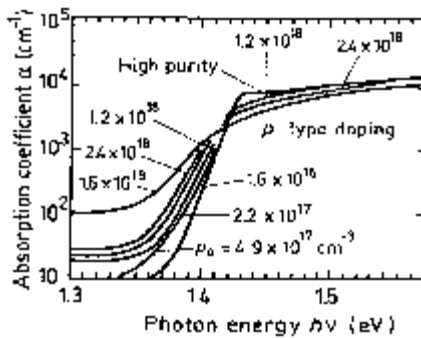
Intrinsic absorption coefficient near the intrinsic absorption edge for different temperatures.

([Sturge \[1962\]](#)).

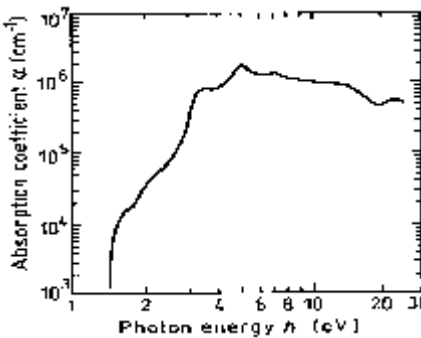
A ground state Rydberg energy $R_{X1} = 4.2$ meV



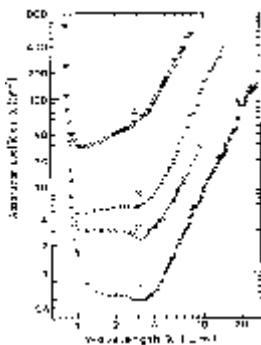
Intrinsic absorption edge at 297 K at different doping levels. *n*-type doping
(Casey et al. [1975]).



Intrinsic absorption edge at 297 K at different doping levels. *p*-type doping
(Casey et al. [1975]).



The absorption coefficient versus photon energy from intrinsic edge to 25 eV.
(Casey et al. [1975]).

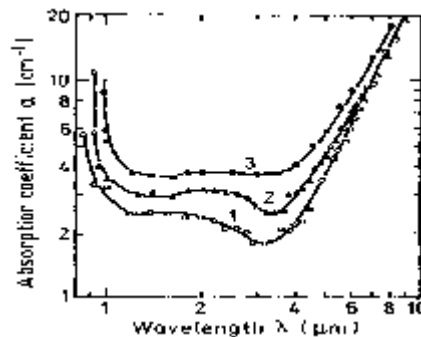


Free carrier absorption versus wavelength at different doping levels, 296 K

(Spitzer and Whelan [1959]).

Conduction electron concentrations are:

1. $1.3 \cdot 10^{17} \text{ cm}^{-3}$; 2. $4.9 \cdot 10^{17} \text{ cm}^{-3}$; 3. 10^{18} cm^{-3} ; 4. $5.4 \cdot 10^{18} \text{ cm}^{-3}$



Free carrier absorption versus wavelength at different temperatures.

$n_0 = 4.9 \cdot 10^{17} \text{ cm}^{-3}$ (Spitzer and Whelan [1959])

Temperatures are: 1. 100 K; 2. 297 K; 3. 443 K.

At 300 K

For $\lambda \sim 2 \mu\text{m}$ $\alpha = 6 \cdot 10^{-18} n_0 \text{ (cm}^{-1}\text{)}$ (n_0 - in cm^{-3})

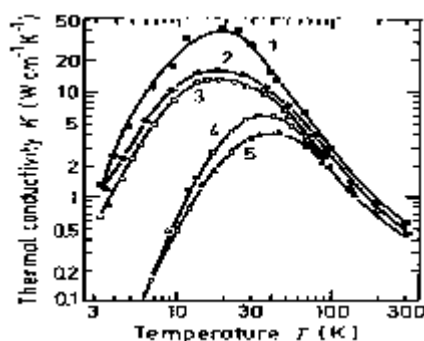
For $\lambda > 4 \mu\text{m}$ and $10^{17} < n_0 < 10^{18} \text{ cm}^{-3}$ $\alpha = 7.5 \cdot 10^{-20} n_0 \cdot \lambda^3 \text{ (cm}^{-1}\text{)}$ (n_0 - in cm^{-3} , λ - μm)



GaAs - Gallium Arsenide

Thermal properties

Bulk modulus	$7.53 \cdot 10^{11} \text{ dyn cm}^{-2}$
Melting point	1240 °C
Specific heat	$0.33 \text{ J g}^{-1} \text{ °C}^{-1}$
Thermal conductivity	$0.55 \text{ W cm}^{-1} \text{ °C}^{-1}$
Thermal diffusivity	$0.31 \text{ cm}^2 \text{ s}^{-1}$
Thermal expansion, linear	$5.73 \cdot 10^{-6} \text{ °C}^{-1}$

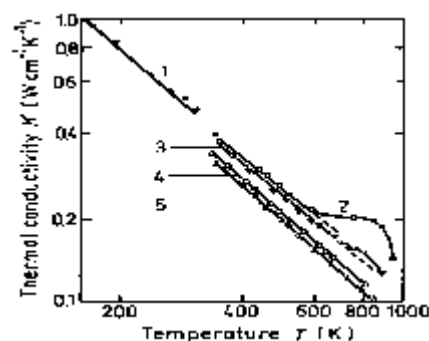


Temperature dependence of thermal conductivity

n-type sample, $n_0 \text{ (cm}^{-3}\text{)}$: 1. 10^{16} ; 2. $1.4 \cdot 10^{16}$; 3. 10^{18} ;

p-type sample, $p_0 \text{ (cm}^{-3}\text{)}$: 4. $3 \cdot 10^{18}$; 5. $1.2 \cdot 10^{19}$.

([Carlson et al \[1965\]](#)).

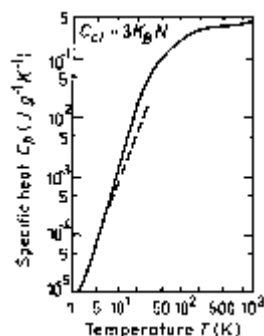


Temperature dependence of thermal conductivity (for high temperature)

n-type sample, $n_0 \text{ (cm}^{-3}\text{)}$: 1. $7 \cdot 10^{15}$; 2. $5 \cdot 10^{16}$; 3. $4 \cdot 10^{17}$; 4. $8 \cdot 10^{18}$;

p-type sample, $p_0 \text{ (cm}^{-3}\text{)}$: 5. $6 \cdot 10^{19}$.

([Blakemore \[1982\]](#)).



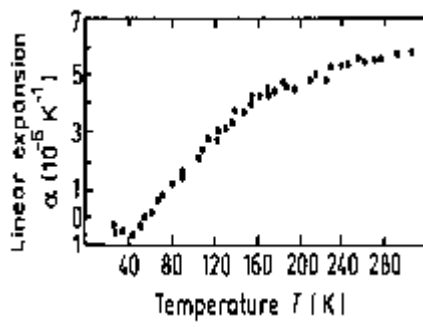
Temperature dependence of specific heat at constant pressure C_{cl} =

$3k_B N = 0.345 \text{ J g}^{-1} \text{ °C}^{-1}$.

N is the number of atoms in 1 g of GaAs.

Dashed line: $C_p = (4 \cdot 10^{-2} C_{cl} / 5 \cdot 10^{-3}) \cdot T^3$ for $T_0 = 345 \text{ K}$.

([Blakemore \[1982\]](#)).



Temperature dependence of linear expansion coefficient •
 ([Novikova\[1961\]](#)).

Melting point	$T_m=1513 \text{ K}$
For $0 < P < 45 \text{ kbar}$	$T_m= 1513 - 3.5P$ (P in kbar)
Saturated vapor pressure (in Pascals)	
1173 K	1
1323 K	100



GaAs - Gallium Arsenide

Mechanical properties, elastic constants, lattice vibrations

[Basic Parameter](#)

[Elastic constants](#)

[Acoustic Wave Speeds](#)

[Phonon frequencies](#)

Basic Parameter

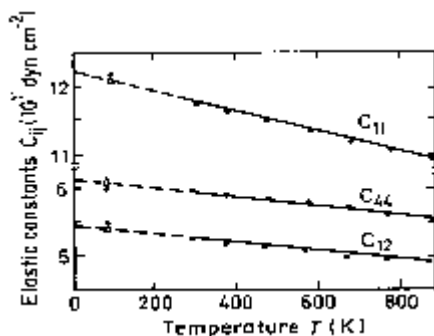
Bulk modulus	$7.53 \cdot 10^{11} \text{ dyn cm}^{-2}$
Density	5.317 g cm^{-3}
Hardness on the Mohs scale	between 4 and 5
Surface microhardness (using Knoop's pyramid test)	750 kg mm^{-2}
Cleavage plane	{110}
Piezoelectric constant	$e_{14} = -0.16 \text{ C m}^{-2}$

Elastic constants 300 K.

$$C_{11} = 11.90 \cdot 10^{11} \text{ dyn/cm}^2$$

$$C_{12} = 5.34 \cdot 10^{11} \text{ dyn/cm}^2$$

$$C_{44} = 5.96 \cdot 10^{11} \text{ dyn/cm}^2$$



Temperature dependences of elastic constants.

For $0 < T < T_m = 1513 \text{ K}$ (in units of $10^{11} \text{ dyn cm}^{-2}$)

$$C_{11} = 12.17 - 1.44 \cdot 10^{-3} T$$

$$C_{12} = 5.46 - 0.64 \cdot 10^{-3} T$$

$$C_{44} = 6.16 - 0.70 \cdot 10^{-3} T$$

(Burenkov et al. [1973])

For T = 300 K

$$\text{Bulk modulus (compressibility}^{-1}) B_s = 7.53 \cdot 10^{11} \text{ dyn/cm}^2$$

$$\text{Shear modulus } C' = 3.285 \cdot 10^{11} \text{ dyn/cm}^2$$

$$[100] \text{ Young's modulus } Y_0 = 8.59 \cdot 10^{11} \text{ dyn/cm}^2$$

$$[100] \text{ Poisson ratio } \nu_0 = 0.31$$

Acoustic Wave Speeds

Wave	Wave	Expression for wave speed	Wave speed
------	------	---------------------------	------------

propagation Direction	character		(in units of 10^5 cm/s)
[100]	V _L	$(C_{11}/\rho)^{1/2}$	4.73
	V _T	$(C_{44}/\rho)^{1/2}$	3.35
[110]	V ₁	$[(C_{11}+C_{12}+2C_{44})/2\rho]^{1/2}$	5.24
	V	$V_{ }=V_T=(C_{44}/\rho)^{1/2}$	3.35
	V _{t⊥}	$[(C_{11}-C_{12})/2\rho]^{1/2}$	2.48
[111]	V _{1'}	$[(C_{11}+2C_{12}+4C_{44})/3\rho]^{1/2}$	5.4
	V _{t'}	$[(C_{11}-C_{12}+C_{44})/3\rho]^{1/2}$	2.8

Phonon frequencies

(in units of 10^{12} Hz) ([Waugh and Dolling \[1963\]](#))

- TO(•) 8.02 • LO (X) 7.22
- LO(•) 8.55 • TA(L) 1.86
- TA(X) 2.36 • LA(L) 6.26
- LA(X) 6.80 • TO(L) 7.84
- TO(X) 7.56 • LO(L) 7.15



GaAs - Gallium Arsenide

References:

- Levinshtein M.E., S.L. Rumyantsev *Handbook Series on Semiconductor Parameters*, vol.1, M. Levinshtein, S. Rumyantsev and M. Shur, ed., World Scientific, London, 1996, pp. 77-103.
 - Dargys A. and J. Kundrotas *Handbook on Physical Properties of Ge, Si, GaAs and InP*, Vilnius, Science and Encyclopedia Publishers, 1994
-
- Aspnes, D. E., *Surface Sci.* **132**, 1-3 (1983) 406-421.
 - Bareikis, V., F. Galdikas, R. Milisyte, and V. Viktoravicius, *Proc. 5th Conf. on Noise in Physical Systems*, Bad Nauheim, West Germany, Mar. 1978, p. 212.
 - Blakemore, J. S., *J. Appl. Phys.* **53**, 10 (1982) R123-R181.
 - Burenkov, Yu. A., Yu. M. Burdukov, S. Yu. Davidov, and S. P. Nikanorov, *Sov. Phys. Solid State* **15**, 6 (1973) 1175-1177.
 - Carlson, R. O., G. A. Slack, and S. J. Silverman, *J. Appl. Phys.* **36**, 2 (1965) 505.
 - Casey, H. C., D. D. Sell, and K. W. Wecht, *J. Appl. Phys.* **46**, 1 (1975) 250.
 - Dalal, V. L., A. B. Dreeben, and A. Triano, *J. Appl. Phys.* **42**, 7 (1971) 2864-2867.
 - de Murcia, M., D. Gasquet, A. Elamri, J. P. Nougier, and J. Vanbremeersch, *IEEE Trans. Electron. Dev.* **ED-38**, 11 (1991) 2531-2539.
 - Dmitriev, A. P., M. P. Mikhailova, and I. N. Yassievich, *Phys. Status Solidi (B)* **140**, 1(1987) 9-137.
 - Fauquemberge, R., J. Zimmermann, A. Kaszynski, and E. Constant, *J. Appl. Phys.* **51**, 2 (1980) 1065-1071.
 - Hilsum, C., *Electron. Lett.* **10**, 13 (1974) 259-260. Joshi, R. and R. O. Grendin, *Appl. Phys. Lett.* **54**, 24 (1989) 2438-2439.
 - Kyuregyan, A. S. and S. N. Yurkov, *Sov. Phys. Semicond.* **23**, 10 (1989) 1126-1132.
 - Milnes, A. G., *Deep Impurities in Semiconductors*, John Wiley and Sons, N.Y., 1973. Novikova, S. I., *Sov. Phys. Solid State* **3**, 1 (1961) 129.
 - Pearsall, T. P., F. Capasso, R. E. Nahory, M. A. Pallack, and J. Chelikowsky, *Solid State Electron.* **21**, 1 (1978) 297-302.
 - Phillip, H. R. and H. Ehrenreich, *Phys. Rev.* **129**, 4 (1963) 1550-1560.
 - Pozhela, J. and A. Reklaitis, *Solid State Electron.* **23**, 9 (1980) 927-933.
 - Rees, H. D., *Solid State Commun.* **7**, 2 (1969) 267-269.
 - Rode, D. L., *Semiconductors and Semimetals*, R. K. Willardson and A. C. Beer, eds., *Academic Press*, N.Y., vol. 10, 1975, p. 1.
 - Ruch, J. G. and G. S. Kino, *Phys. Rev.* **174**, 3 (1968) 921-931.
 - Shur, M., *Physics of Semiconductor Devices*, Prentice Hall, 1990.
 - Spitzer, W. G. and J. M. Whelan, *Phys. Rev.* **114**, 1 (1959) 59-63.
 - Stillman, G. E., C. M. Waife, and J. O. Dimmock, *J. Phys. Chem. Solids* **31**, 6 (1970) 1199-1204.
 - Sturge, M. D., *Phys. Rev.* **127**, 3 (1962) 768.
 - Sze, S. M., *Physics of Semiconductor Devices*, John Wiley and Sons, N.Y., 1981.
 - Tiwari, S. and S. L. Wright, *Appl. Phys. Lett.* **56**, 6 (1990) 563-565.
 - Varshni, V. P., *Phys. Status Solidi* **19**, 2 (1967) 459-514; **20**, 1 (1967) 9-36.
 - Waugh, J. L. T. and G. Dolling, *Phys. Rev.* **132**, 6 (1963) 2410.
 - Wiley, J. D., *Semiconductor and Semimetals*, R. K. Willardson and A. C. Beer, eds., *Academic Press*, N.Y., vol. 10, 1975, p. 91.

